SOLAR-TERRESTRIAL-CLIMATE RELATIONS AT AGASSIZ, BRITISH COLUMBIA

by

Paul L. Vaughan
B. Sc. UNB 1995

THESIS SUBMITTED IN PARTIAL FULFILLMENT OF
THE REQUIREMENTS FOR THE DEGREE OF

MASTER OF SCIENCE
Under Special Arrangements

In the
Faculty
of
Science

SIMON FRASER UNIVERSITY

December 2008

PARTIAL COPYRIGHT LICENCE

Title of Thesis/Project/Extended Essays:

SOLAR-TERRESTRIAL-CLIMATE RELATIONS AT AGASSIZ, BRITISH COLUMBIA

Author: ______________________________

(Signature)

Paul L. Vaughan

____

(Date Signed)

APPROVAL

Name: **Paul L. Vaughan**

Degree: **Master of Science Under Special Arrangements**

Title of Thesis: **Solar-Terrestrial-Climate Relations at Agassiz, British Columbia**

Examining Committee:

Chair: **Title and Name**
[Assistant/Associate] Professor of/Department of

Title and Name
Senior Supervisor
[Associate/Assistant] Professor of/Department of ????

Title and Name
Supervisor
[Associate/Assistant] Professor of/Department of ???

Title and Name
[Internal/External] Examiner
[Associate/Assistant] Professor of/Department of???
University (if other than SFU)

Date Defended/Approved:

Abstract

Relationships involving solar, terrestrial, and Agassiz, British Columbia weather summaries are investigated across a spectrum of timescales using a selection of methods including wavelet & time-integrated cross-correlation analyses. Benefits of investigating alternate weather summaries beyond mean temperatures are highlighted. Temperature range indices are shown to be strongly related to geomagnetic aa index across a century-scale epoch (1891-2005) at the timescale of the solar Schwabe (~11 year) cycle. Monthly maximum temperature summaries are shown to be strongly related to cosmic ray flux during a multi-decadal epoch (1953-2005) at the timescales of the solar Schwabe & Hale (~22 year) cycles. Average monthly minimum temperature is shown to be more tightly synchronized with solar & terrestrial variables than are other temperature summaries. Attention is drawn to a seemingly strong phase relationship involving terrestrial polar motion and an index of solar system orbital inertia. Finally, relationships involving terrestrial carbon dioxide concentration are briefly explored.

ACKNOWLEDGEMENTS

I acknowledge those who have been supportive.

TABLE OF CONTENTS

LIST OF FIGURES

LIST OF TABLES

Introduction

A variety of reports from recent years have addressed climate &/or climatic trends in coastal British Columbia &/or the Pacific Northwest of the USA (BC government 2007, 2006, 2004, & 2002; Leung & Qian 2003; Mote 2003; Turner & Clague 1999; Vaccaro 2002; Wade et al. 2001; Walker & Pellatt, 2003; Whitfield et al. 2002 & 2003). While celestial-terrestrial climate influences do not form a core focus in these reports, the BC government climate reports, in particular, fuel curiosity regarding relative trends in minimum & maximum temperatures, topics which are explored in the more general climate literature by Vincent et al. (2005), Karl et al. (1993), Easterling et al. (1997), Vose et al. (2005), del Rio et al. (2007), Mahmoud (2006), and Stone & Weaver (2002, 2003).

Mursula & associates (2008, 2007, 2004, 2003, 2002, 2001, 1999, 1998, 1996), Lundstedt & associates (2007, 2006, 2005), Georgieva & associates (2007, 2006, 2005, 2002, 2000, 1998), Javaraiah (2005, 2003), Kato et al. (2003), Tomes (2005), Juckett (1998), Sakurai (2002), and Krivova & Solanki (2002) explore solar parameters & related periodicities influencing or potentially influencing solar-terrestrial relations. Relationships between terrestrial mean temperature variables and indicators of solar activity reported in the solar-terrestrial relations literature have gleaned considerable attention, particularly with regards to the strong relationships noted at the timescale of the solar Schwabe (~11a) cycle (Cliver et al. 1998; Reid 1987; Landscheidt 1999; White et al. 1997; Scafetta & West 2006; Wilson 1998; Valev 2006).

Evidence of a relationship between terrestrial climate and cosmic ray flux continues to mount in the literature (Usoskin 2007, 2006a; Svensmark 2007a;

Veizer 2005; Palle et al. 2004; Tinsley 2000-2007; Perry 2007; Shaviv et al. 2002-2005). At both heliospheric & terrestrial magnetospheric scales, solar activity modulates cosmic ray flux which induces ionization in the terrestrial atmosphere which in turn, through electrostatic/aerosol interactions, affects cloud condensation nuclei dynamics to influence low-altitude cloud coverage, which has effects such as moderating daytime maximum temperatures. Usoskin & Kovaltsov (2007) caution that "use of global or even zonally averaged data may be misleading" due to strong regional, magnetosphere-related variability in the relationship between cosmic ray flux & low-altitude cloud cover, which may vary on a timescale of centuries & longer.

Keeling & Whorf (1997 & 2000) suggest ocean tide patterns may play a stronger role in global temperature trends than has traditionally been considered possible. They emphasize that tidal cycles do not repeat exactly, even after centuries, and, worthy of note with regards to the present study, they point to an interval early during the 20th century (1900-1945) when the usual dominance of nearly decadal oscillations in global average temperature was interrupted to a considerable extent by a roughly 6 year signal they believe may, in part, be due to correspondingly distinct tidal event periodicity patterns between 1899 & 1947.

Vondrak (1999), Gross (2005), Brzezinski (2003), and Stuck et al. (2005) report on proposed causes of & periodicities appearing in earth orientation parameters, including polar position. Kolaczek et al. (2003) and Lehmann et al. (2008) report relationships between earth orientation parameters and the El Nino Southern Oscillation (ENSO) phenomenon, which Newman et al. (2003) suggest directly forces the Pacific Decadal Oscillation (PDO). Relying on wavelet analysis, Yndestad (2006) suggests a strong relationship between polar position, which he considers an indicator of the lunar nodal cycle, and arctic temperature series, but McKinnell & Crawford (2007) report only a weak relationship between the lunar nodal cycle and temperatures in the region of the northeastern Pacific Ocean. Currie (1996), who employs filtering techniques commonly used in electrical engineering, seems to contend that significant lunisolar components are detectable in a very wide variety of terrestrial time series, including virtually all climate series. He investigates terrestrial geographic sites individually (thousands of them) and cautions that zonal &/or global averaging masks locally-detectable signals that are intermittently out-of-phase with those at different locations, even ones relatively nearby.

Jose (1965), Landscheidt (1999), Charvatova (2009, 2007, 2000), Juckett (2000), Palus et al. (2007), Bucha et al. (1985), Alexander et al. (2007), Freeman & Hasling (2004), and Wilson et al. (2008) consider terrestrial climate links with solar orbital dynamics &/or solar activity indices. Landscheidt (2002, 2001, 2000, 1999) pointed out the coincident timing of extrema in solar orbital summaries and extrema in a variety of terrestrial climate phenomena, including ENSO, the PDO, and the North Atlantic Oscillation (NAO).

Haigh (2007) and MacKey (2007) provide recent literature reviews of solar-terrestrial relations from relatively conservative & relatively liberal perspectives, respectively.

Keeling & Whorf (1997) admit that research into cycles in climate "does not have a good reputation" in some scientific circles, due to exceptions & inconsistencies in noted patterns. Economist Edward R. Dewey (1970) suggested, "The study of cycles reveals to us our ignorance, and is therefore very disturbing to people whose ideas are crystallized." Casdagli (1991) stresses the extraordinary diversity of behaviours which can be exhibited by nonlinear dynamical systems and Currie (1996) suggests that "on decadal and duodecadal time-scales the spectrum of climate is signal-like rather than noise-like, as radically assumed by statisticians and mathematicians the past 70 years." Palus & Novotna (2007) suggest that even very weak interactions can be detected by studying the instantaneous phase relations of oscillatory processes. They go on to say, "We believe that the synchronization analysis will help to uncover mechanisms of the tropospheric responses to the geomagnetic activity and to contribute to better understanding of the solar-terrestrial relations and their role in the climatic change."

Ecologists Allen & Hoekstra (1991 & 1992) offer a framework for conceptualizing & investigating scale-dependent pattern & process as influenced by spatiotemporal heterogeneity. With the same theme in mind, geographers Fotheringham & Rogerson (1993) assert that scale-dependency "... presents us with the challenge of reporting on the reliability of parameter estimates in the light of changes in scale ..." The scale-cognizant paradigm has exerted a fundamental & dominating influence on the multiscale approach employed in the present research.

A considerable proportion of investigations of celestial-terrestrial-climate linkages:

a) investigate multi-annual phenomena only with annual-resolution data.

b) limit the presentation of data & estimates to only selected timescales, rather than empowering audiences with access to patterns from across a broader context.

c) focus more on means than on minima, maxima, ranges, &/or other summaries.

The preceding, all considered in conjunction, suggested an array of interesting research opportunities, some of which have already been pursued. This document presents a selection of the early results.

Study Variables

Geomagnetic aa Index

The geomagnetic aa index (**aa**) is a measure of the sun's coronal magnetic field strength (magnetic flux density) as mediated through the interplanetary magnetic field (IMF) and integrated by the Earth's magnetosphere. According to Palus & Novotna (2007), "The aa-index is defined by the average, for each 3-hour period, of the maximum of magnetic elements from two near-antipodal mid-latitude stations in Australia (Melbourne) and England (Greenwich)." There are other indices of geomagnetic activity, but an important advantage of the aa index is that its record extends back to 1868 and is homogenous.

Monthly aa index measurements were downloaded from a USA National Oceanic and Atmospheric Administration (NOAA) website *(ftp://ftp.ngdc.noaa.gov/STP/SOLAR_DATA/RELATED_INDICES/AA_INDEX/AA_MONTH)*.

The square root & logarithm (base 2, for ease of interpretation) of this variable were found to ease analyses. There was a lack of strong evidence that one of these transforms was broadly superior to the other.

Sunspot Numbers

Sunspot numbers (**R**) are indices of solar coronal magnetic activity & potential based on inspection of the visible solar disk. Reliable data go back as far as 1749.

Monthly sunspot numbers were downloaded from a USA National Oceanic and Atmospheric Administration (NOAA) website *(ftp://ftp.ngdc.noaa.gov/STP/SOLAR_DATA/SUNSPOT_NUMBERS/MONTHLY)*.

The logarithm of this variable (plus 1 to avoid log(0)) was found to ease analyses.

Cosmic Ray Flux

A shower of energetic particles known as cosmic rays reaches Earth from both the sun & extrasolar sources, inducing ionization in the terrestrial atmosphere through collisions with atmospheric molecules. Cosmic ray induced ionization is purported to be responsible for a variety of complex microphysical atmospheric processes, many of which are not yet fully understood.

The monthly cosmic ray flux (**CRF**) series for Huancayo, Peru / Haleakala, Hawaii, which dates back to 1953 and is based on neutron monitor counting rates, was downloaded from a USA National Oceanic and Atmospheric Administration (NOAA) website *(ftp://ftp.ngdc.noaa.gov/STP/SOLAR_DATA/COSMIC_RAYS/huancayo.tab)*.

Polar Position

The terrestrial rotation axis wobbles & drifts over time, relative to a geocentric frame based on the terrestrial crust.

Polar position x & y ($\mathbf{P_x}$ & $\mathbf{P_y}$) coordinate time series were downloaded from the International Earth Rotation & Reference Systems Service (IERS) website *(http://hpiers.obspm.fr/eoppc/eop/eopc01/eopc01.1846-1899)*. Monthly-timescale coordinates had to be estimated by interpolation since polar position measurements number 10 per year before 1890 and 20 per year since then.

Atmospheric Carbon Dioxide Concentration

The Mauna Loa, Hawaii atmospheric carbon dioxide ($\mathbf{CO_2}$) concentration monthly time series was downloaded from a USA National Oceanic and

Atmospheric Administration (NOAA) website

(ftp://ftp.cmdl.noaa.gov/ccg/co2/trends/co2_mm_mlo.txt).

Solar Inertia

Characterizations of solar orbital inertia (**SI**), as influenced by the jovian or gas giant planets, Jupiter, Saturn, Uranus, & Neptune, were based on crudely simplified circular orbits in a single plane, with 1960 solar ecliptic coordinates coordinated with coordinates provided by an online NASA calculator *(http://cohoweb.gsfc.nasa.gov/helios/planet.html)*.

Agassiz, British Columbia (BC) Weather

Preliminary investigations focused on other sites in the Vancouver, BC area, but the Agassiz weather station, which is situated just over 100km east of Vancouver & the Strait of Georgia, where the Fraser Valley narrows between the Coast Mountains to the north & the Cascade Mountains to the south heading inland, was found to have a record of superior quality for the present study.

Weather records from Environment Canada for Agassiz, BC *(http://www.climate.weatheroffice.ec.gc.ca/climateData/bulkdata_e.html?timeframe=3&Prov=XX&StationID=707&Year=1889&Month=1&Day=1&format=csv&type=mly)* show only a handful of missing records. Temperature records for Agassiz go back to August 1891. The few Vancouver area records that go back further show large quantities of missing records.

The few missing temperature data for Agassiz since August 1891 were estimated via very strong relationships with nearby stations (Chilliwack & New Westminster, BC, in order of preference as dictated by correlations & residuals and depending upon record availability).

Precipitation records for Agassiz go back a little further than temperature records, but estimating missing precipitation data for the early portion of the record proved problematic due to gaps in records at nearby stations and large residuals found in relationships with precipitation records from further away, so data from before August 1891 were omitted from analyses.

The weather variables of focus in the present study are:

1) **TMax** = monthly average maximum temperature
2) **TMin** = monthly average minimum temperature
3) **TMean** = monthly average temperature (defined by convention as the average of TMax & TMin)
4) **XTMax** = monthly extreme maximum temperature
5) **XTMin** = monthly extreme minimum temperature
6) **PPT** = precipitation

   The square root, cubed root, & logarithmic transforms of this variable were found to ease analyses.

7) **TRange = TR** = TMax - TMin = monthly average temperature range

   This variable can also be expressed as TMax / TMin (using absolute temperatures in degrees Kelvin) with little change to the results of analyses.

   Although working with the logarithm (base 2, for ease of interpretation) of the TRange variable results in a more symmetrical univariate distribution, this approach has almost negligible effects on the results of analyses.

8) **XTRange = XTR** = XTMax - XTMin = monthly extreme temperature range

Table 1 summarizes the gap-free record intervals that were available for the present study according to combinations of solar-terrestrial-climate variables.

Table 1. Study record intervals available by combination of study variables.

Combination of Variables	Record Interval Available for Combination
R, **aa**, **polar position**, **SI**, Agassiz weather	August **1891** - May **2005**
CRF, R, aa, polar position, SI, Agassiz weather	January **1953** - May **2005**
CO_2, CRF, R, aa, polar position, SI, Agassiz weather	March **1958** - May **2005**

Relationships

Illustrating Complex Relationships Involving Solar Variables

It is important to begin this communication by emphasizing that relationships between variables involving complex acoustic feedbacks, analogous to the echoes of a whistling train passing through a complex mountainous landscape, and/or intermittent periods of phase drift, analogous to water flowing in-to and out-of a reservoir at differing variable rates reflecting different processes that equal-out in rate quasi-periodically, may present challenges to comprehension-paradigms governed primarily by linear logic.

To further reinforce this point while also introducing an important relationship, the relationship between geomagnetic aa index and sunspot numbers is presented. Similarities between the aa & R time series are apparent (Figure 1), but a variable timescale view (Figure 2) makes the similarities more apparent. Wavelet phase plots (Figure 2, 1st column) for aa & R are strikingly similar and the cross-wavelet phase-plot (Figure 2e) verifies cyclically bounded asynchrony. Cross-correlation analysis (Figure 2f) reveals the gain in correlation achieved by integrating (over time) across the dominant cycles revealed by cross-wavelet analysis. A sequence of conventional scatterplots (Figure 2g-i) further reinforces the change in perspective gained by integrating over the ~11a cycles of bounded asynchrony.

The relationships of the aa & R time series with the CRF time series, which appears in the lower panel of Figure 1, involve an even/odd ~11a Schwabe cycle morphology related to solar magnetic polarity reversals roughly half-way through ~22a Hale solar magnetic cycle. CRF is addressed in more detail below.

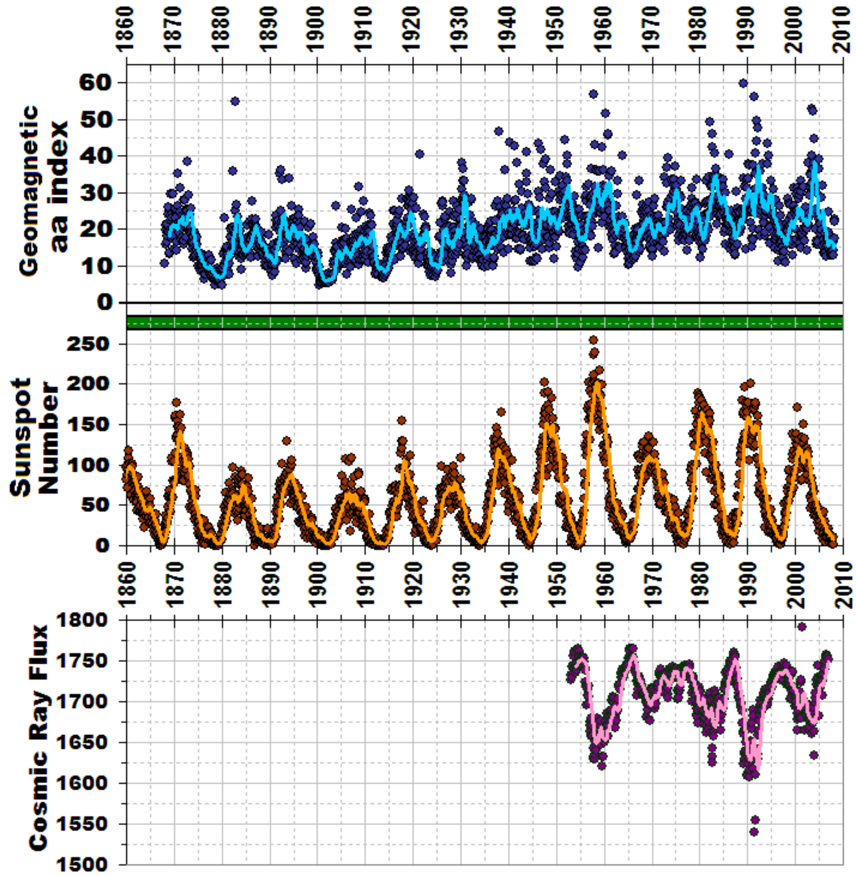

Figure 1. Time series of average monthly geomagnetic aa index <aa> (nT (nano-Teslas)), sunspot number <R>, and galactic cosmic ray flux <CRF> (average neutron counting rates per hour; Huancayo, Peru / Haleakala, Hawaii series; cutoff rigidity ~12.915GV (1980)) with 1 year moving averages superimposed.

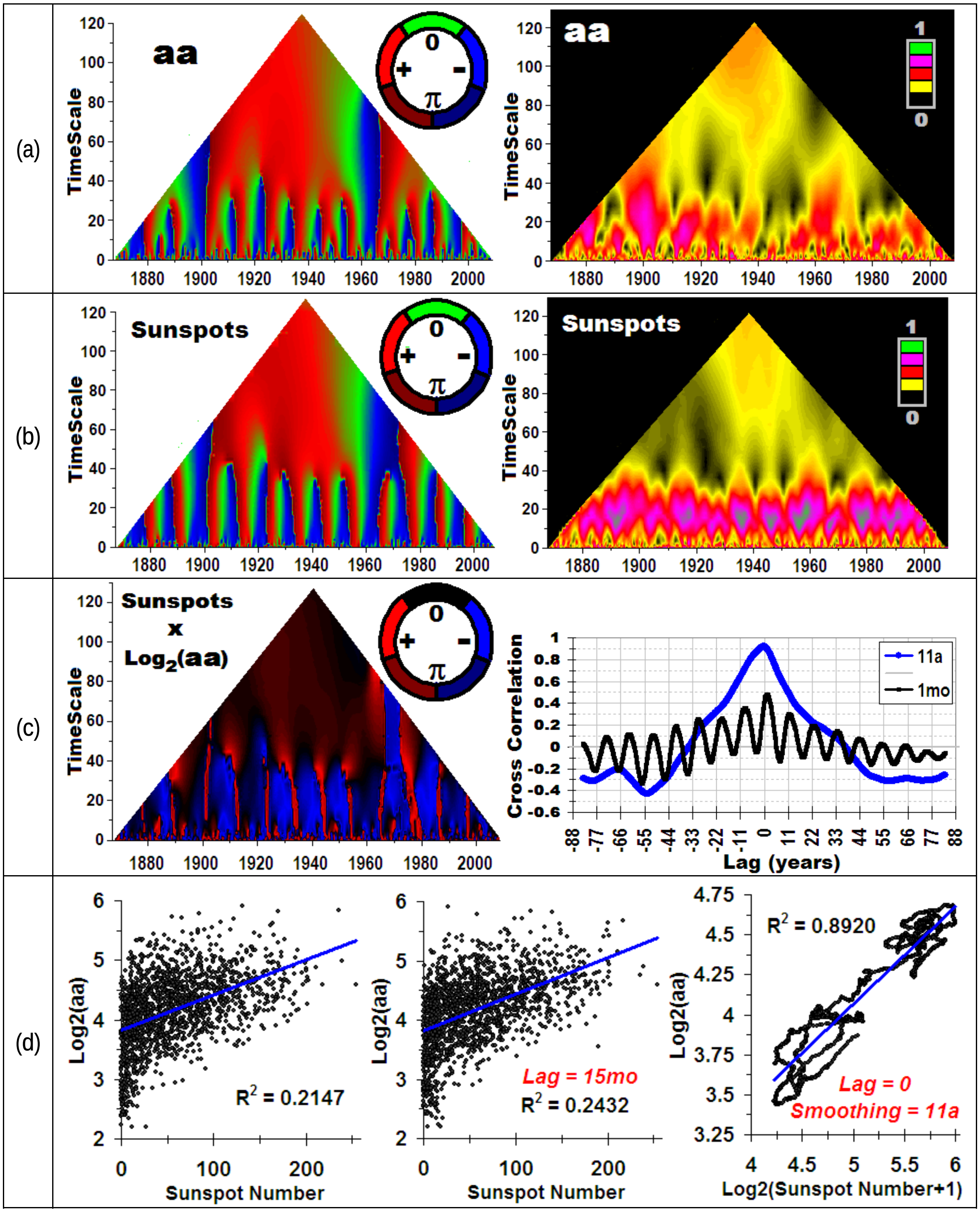

Figure 2. Wavelet transforms of average monthly solar activity indices (1868-2007). (a) Geomagnetic aa index phase & power. (b) Sunspot number phase & power. (c) Cross-wavelet phase difference and cross-correlation of sunspot number with geomagnetic aa index. (d) Scatterplot; best-lag scatterplot (Lag = 15 months); and best-lag scatterplot with 11 year bandwidth smoothing and a log-transform of sunspot number. Timescale is in years.

Relationship of Geomagnetic aa Index with Agassiz, BC Temperature Summaries

A crude preliminary investigation revealed:

1) interesting rough parallels between 11a-smoothed geomagnetic aa index and the negative of Agassiz, BC temperature range (Figure 3a).

2) a provocative matrix of roughly harmonic best-lags stemming from the cross-correlation functions of time series smoothed to varying extents based upon a very loose & subjective exploratory criterion of smoothing until "not too spiky" (Figure 3b).

(a)

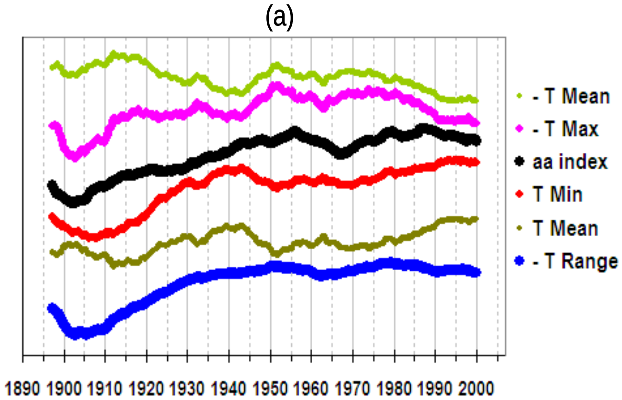

(b)

Smoothed	SqRt.aa	TMax	TMean	TMin	Log2.TR	XTMax	XTMin	XTR	SqRt.PPT
SqRt.aa		1	-3	0	0	-49	0	0	-24
TMax	-1		-12	-6	0	2	-12	0	-25
TMean	3	12		0	7	0	0	-1	-24
TMin	0	6	0		1	-26	0	0	-25
Log2.TR	0	0	-7	-1		-26	-6	0	-24
XTMax	49	-2	0	26	26		0	50	-3
XTMin	0	12	0	0	6	0		0	-23
XTR	0	0	1	0	0	-50	0		-24
SqRt.PPT	24	25	24	25	24	3	23	24	

Figure 3. (a) 11-year-smoothed time series of Agassiz, BC temperature summaries and geomagnetic aa index (1891-2005). The series are linearly shifted & scaled to facilitate comparative viewing. Note also that it is the *negative* of some temperature variables that is shown. (b) Matrix of best-lags from cross-correlation functions for select pairs of study variables initially smoothed according to a loose & subjective preliminary-investigation criterion of looking "not too spiky", for the purposes of early exploration.

This led to more systematic investigations, including one of the relationship of Agassiz, BC temperature range with geomagnetic aa index across a variety of smoothing bandwidths (Figure 4), which was next expanded to include other temperature summaries, including alternate summaries of temperature range (Tables 2 & 3).

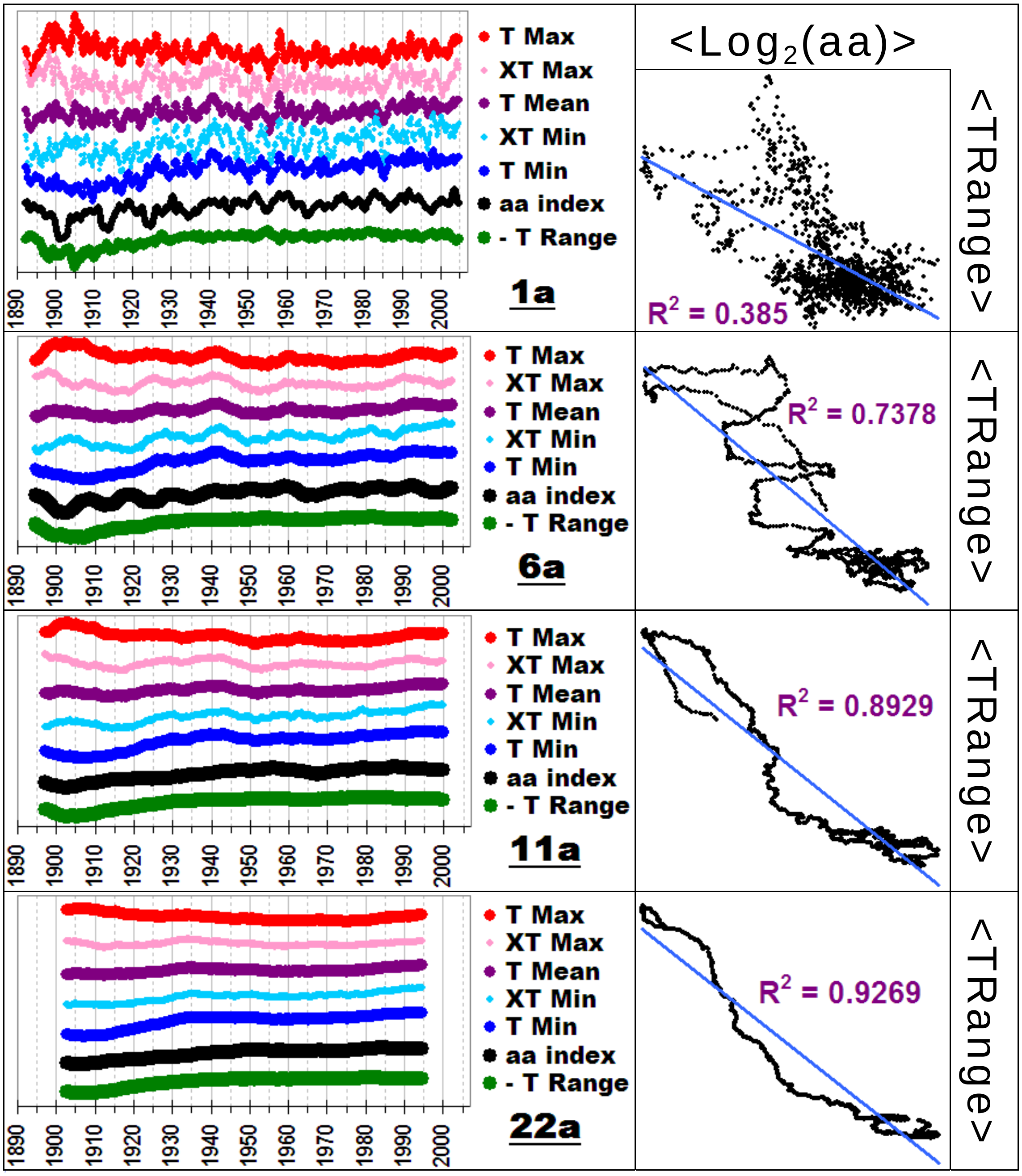

Figure 4. Time series (1891-2005) of average monthly geomagnetic aa index <Log$_2$(aa)> and Agassiz, BC temperature variables at moving-average smoothing-bandwidths of 1 year, 6 years, 11 years, and 22 years. The series are linearly shifted & scaled to facilitate comparative viewing. Note that it is the *negative* of <TRange> that is shown in the *left* column. <TRange> is the study variable most closely associated with aa index. Scatterplots of <TRange> vs. <Log$_2$(aa)> (one for each smoothing bandwidth) appear down the right column.

Table 2. Relationships (1891-2005) of selected monthly weather summaries with average monthly geomagnetic aa index <Log_2(aa)> at a selection of smoothing bandwidths.

	TMean	TMax	TMin	TRange = TMax - TMin	TMax - 1.557*TMin	XTMax - TMin
1 mo	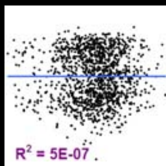 $r^2 = 5E-07$	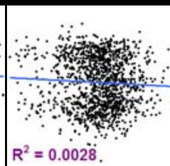 $r^2 = 0.0028$	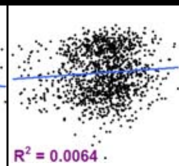 $r^2 = 0.0064$	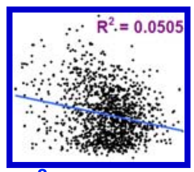 **$r^2 = 0.0505$**	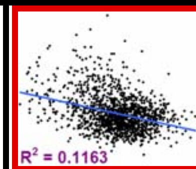 $r^2 = 0.1163$	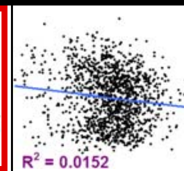 $r^2 = 0.0152$
6 mo	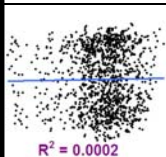 $r^2 = 0.0002$	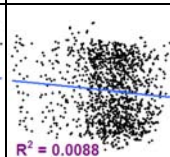 $r^2 = 0.0088$	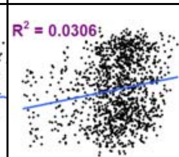 $r^2 = 0.0306$	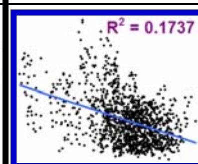 **$r^2 = 0.1737$**	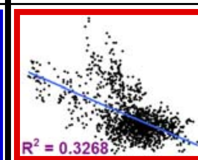 $r^2 = 0.3268$	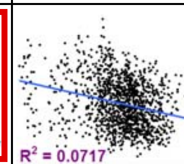 $r^2 = 0.0717$
1 a	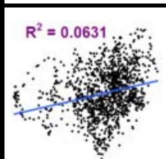 $r^2 = 0.0631$	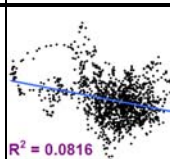 $r^2 = 0.0816$	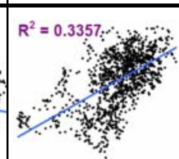 $r^2 = 0.3357$	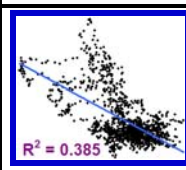 $r^2 = 0.3850$	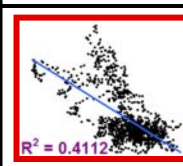 $r^2 = 0.4112$	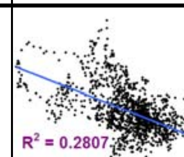 $r^2 = 0.2807$
6 a	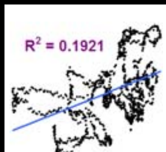 $r^2 = 0.1921$	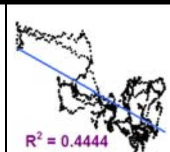 $r^2 = 0.4444$	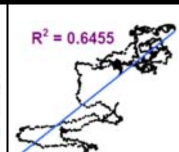 $r^2 = 0.6455$	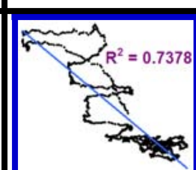 $r^2 = 0.7378$	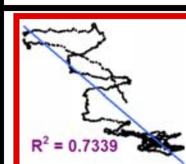 $r^2 = 0.7339$	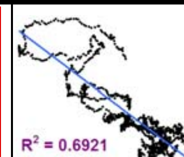 **$r^2 = 0.6921$**
11 a	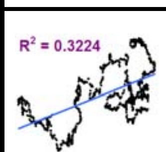 $r^2 = 0.3224$	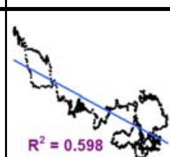 $r^2 = 0.5980$	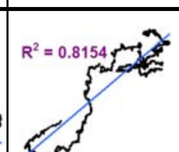 $r^2 = 0.8154$	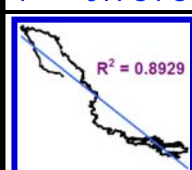 **$r^2 = 0.8929$**	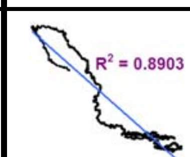 **$r^2 = 0.8903$**	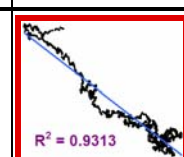 $r^2 = 0.9313$
22 a	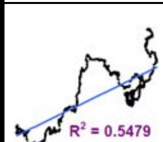 $r^2 = 0.5479$	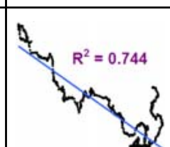 $r^2 = 0.7440$	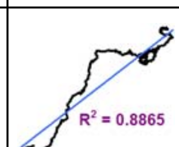 $r^2 = 0.8865$	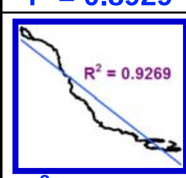 **$r^2 = 0.9269$**	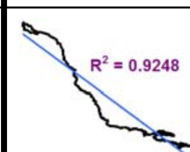 **$r^2 = 0.9248$**	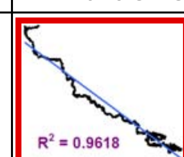 $r^2 = 0.9618$

Table 3. Best-Lag relationships (1891-2005) of selected monthly weather summaries with average monthly geomagnetic aa index <Log$_2$(aa)> at a selection of smoothing bandwidths. Best-Lags were determined via the cross-correlation function.

	TMean	TMax	TMin	TRange = TMax - TMin	TMax - 1.557*TMin	XTMax - TMin
1 mo	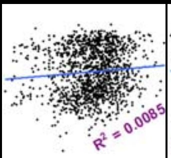 *Lag = -6 mo* r^2 = 0085	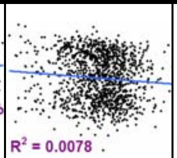 *Lag = 46 mo* r^2 = 0.0078	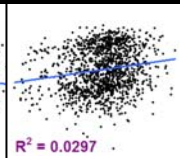 *Lag = 42 mo* r^2 = 0.0297	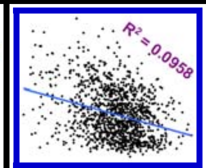 *Lag = 39 mo* **r^2 = 0.0958**	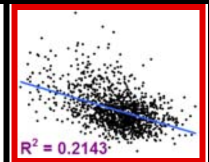 *Lag = 39 mo* r^2 = 0.2143	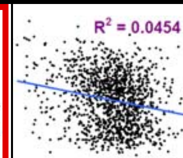 *Lag = 38 mo* r^2 = 0.0454
6 mo	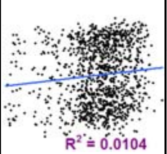 *Lag = **-9.5** a* r^2 = 0.0104	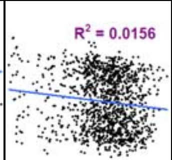 *Lag = 36 mo* r^2 = 0.0156	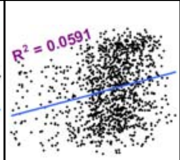 *Lag = 30 mo* r^2 = 0.0591	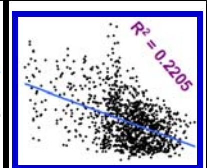 *Lag = 36 mo* **r^2 = 0.2205**	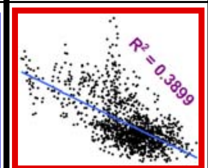 *Lag = 38 mo* r^2 = 0.3899	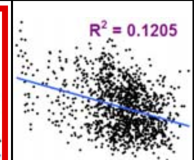 *Lag = 37 mo* r^2 = 0.1205
1 a	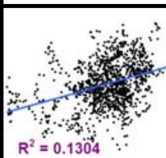 *Lag = **-9.5** a* r^2 = 0.1304	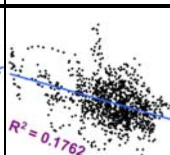 *Lag = 38 mo* r^2 = 0.1762	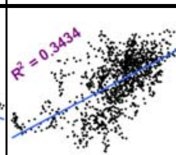 *Lag = -6 mo* r^2 = 0.3434	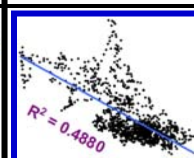 *Lag = 34 mo* r^2 = 0.4880	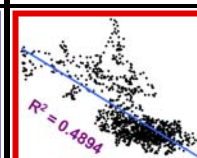 *Lag = 34 mo* r^2 = 0.4894	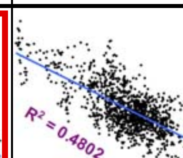 *Lag = 36 mo* **r^2 = 0.4802**
6 a	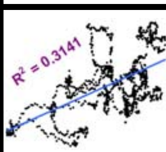 *Lag = **-8.42** a* r^2 = 0.3141	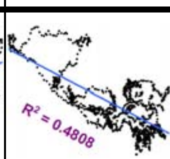 *Lag = 23 mo* r^2 = 0.4808	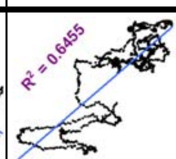 ***Lag = 0*** r^2 = 0.6455	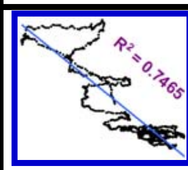 *Lag = 12 mo* **r^2 = 0.7465**	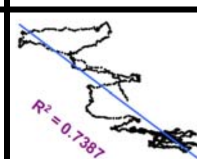 *Lag = 8 mo* **r^2 = 0.7387**	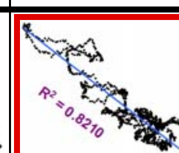 *Lag = 34 mo* r^2 = 0.8210
11 a	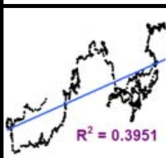 *Lag = **-6.75** a* r^2 = 0.3951	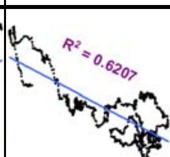 *Lag = 11 mo* r^2 = 0.6207	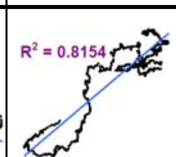 ***Lag = 0*** r^2 = 0.8154	 ***Lag = 0*** **r^2 = 0.8929**	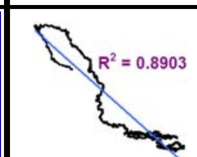 ***Lag = 0*** **r^2 = 0.8903**	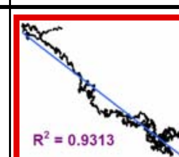 ***Lag = 0*** r^2 = 0.9313
22 a	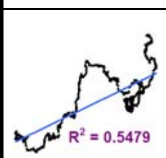 ***Lag = 0*** r^2 = 0.5479	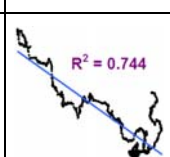 ***Lag = 0*** r^2 = 0.7440	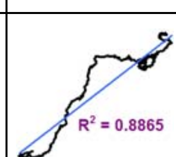 ***Lag = 0*** **r^2 = 0.**8865	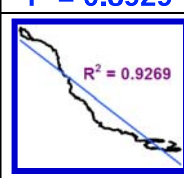 ***Lag = 0*** **r^2 = 0.9269**	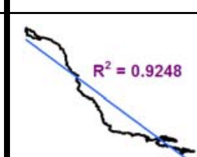 ***Lag = 0*** **r^2 = 0.9248**	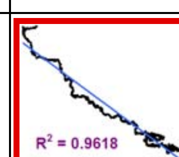 ***Lag = 0*** r^2 = 0.9618

At this point, it is convenient to introduce angled brackets **< >** to notationally indicate time-integration via smoothing (simple box-kernel averaging).

Although both <TMax> and <TMin> are significantly correlated with <Log_2(aa)> at the monthly timescale, the correlations are very small. The contrast <TRange> = <TMax-TMin> is far more strongly correlated with <Log_2(aa)> than are either of <TMax> & <TMin> alone. In addition to <TRange>, two other indices of temperature range are featured for comparison. <TMax-1.557TMin> is seen to be most strongly related to aa index at timescales of 1 year or less, whereas <XTMax-TMin> is strongest at timescales of 11 years & higher. Of the three non-range variables presented, <TMin> is strongest in its relationship with aa index and the blend <TMean> = <(TMax+TMin)/2> is weakest.

Best-lag (based on the cross-correlation function) scatterplots in Table 3 reveal a few highlights beyond what can be gleaned from Table 2:

1) A best-lag in the neighborhood of 39 to 40 months (~3.25a) shows up for all temperature summaries other than <TMean>.
2) <TMin> exhibits the most quickly tightening lag pattern with increasing time-integration.

While Tables 2 & 3 convey a fairly clear outline of geomagnetic aa index correlations (squared) with a selection of temperature summaries across a crude selection of smoothing bandwidths, it is desirable to explore what is happening at intermediate timescales across a slightly expanded set of variables, including an alternate solar variable, sunspot number (Figures 5 & 6).

(a)

(b)

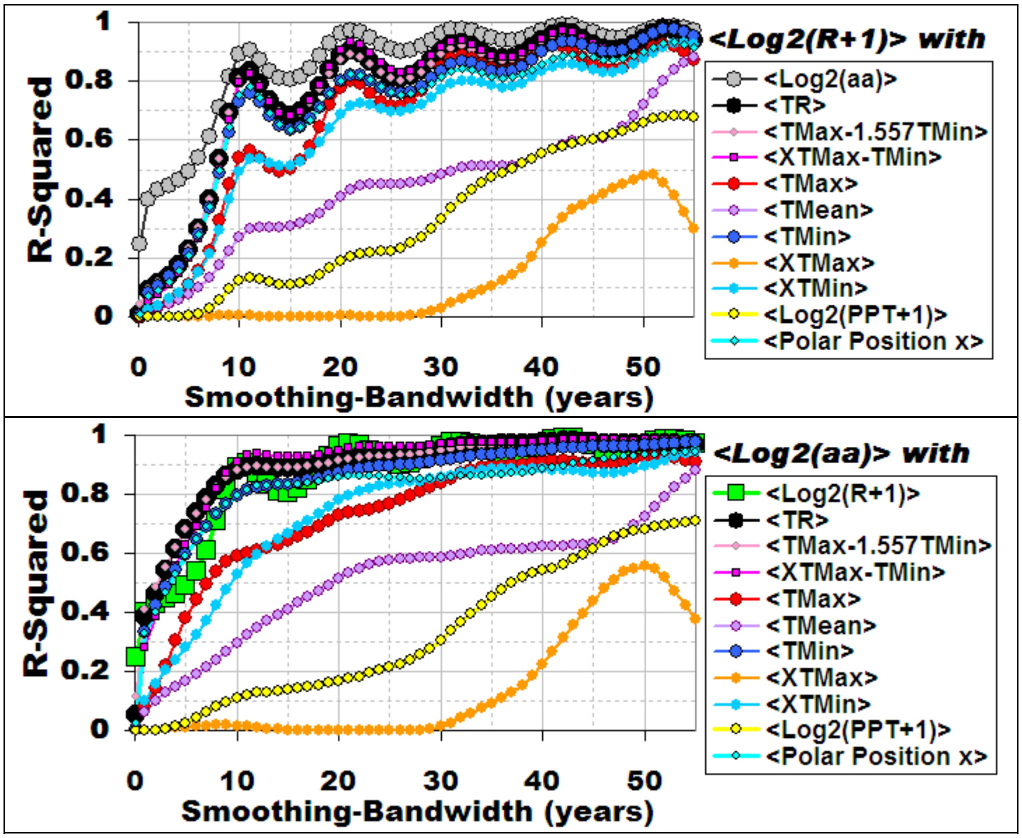

Figure 5. A comparison (1891-2005) of the strengths of the time-integrated relationships (Lag = 0) of (a) average monthly sunspot number $<Log_2(R+1)>$ and (b) average monthly geomagnetic aa index $<Log_2(aa)>$ with a selection of study variables.

A comparison of the strengths of the time-integrated relationships (Lag = 0) of average monthly sunspot number $<Log_2(R+1)>$ (Figure 5a) and average monthly geomagnetic aa index $<Log_2(aa)>$ (Figure 5b) with a selection of study variables makes it clear that the strength of sunspot number relationships notably varies harmonically with time-integration, as evidenced by sags centred on midpoints between successive multiples of ~11 years, and that aa index is almost exclusively more strongly related to all depicted study variables across all levels of time-integration. A major point to note is the substantial degree of aa index superiority over sunspot number in the depicted relationships in-between the Schwabe-resolution resonance nodes. This is, probably in large part, because the aa index captures information about both heliospheric & geomagnetospheric dynamics as experienced at Earth, whereas sunspot number is a less geocentric variable that largely only indicates solar potential, capturing information about neither interplanetary magnetic field (IMF) configuration nor the geomagnetosphere.

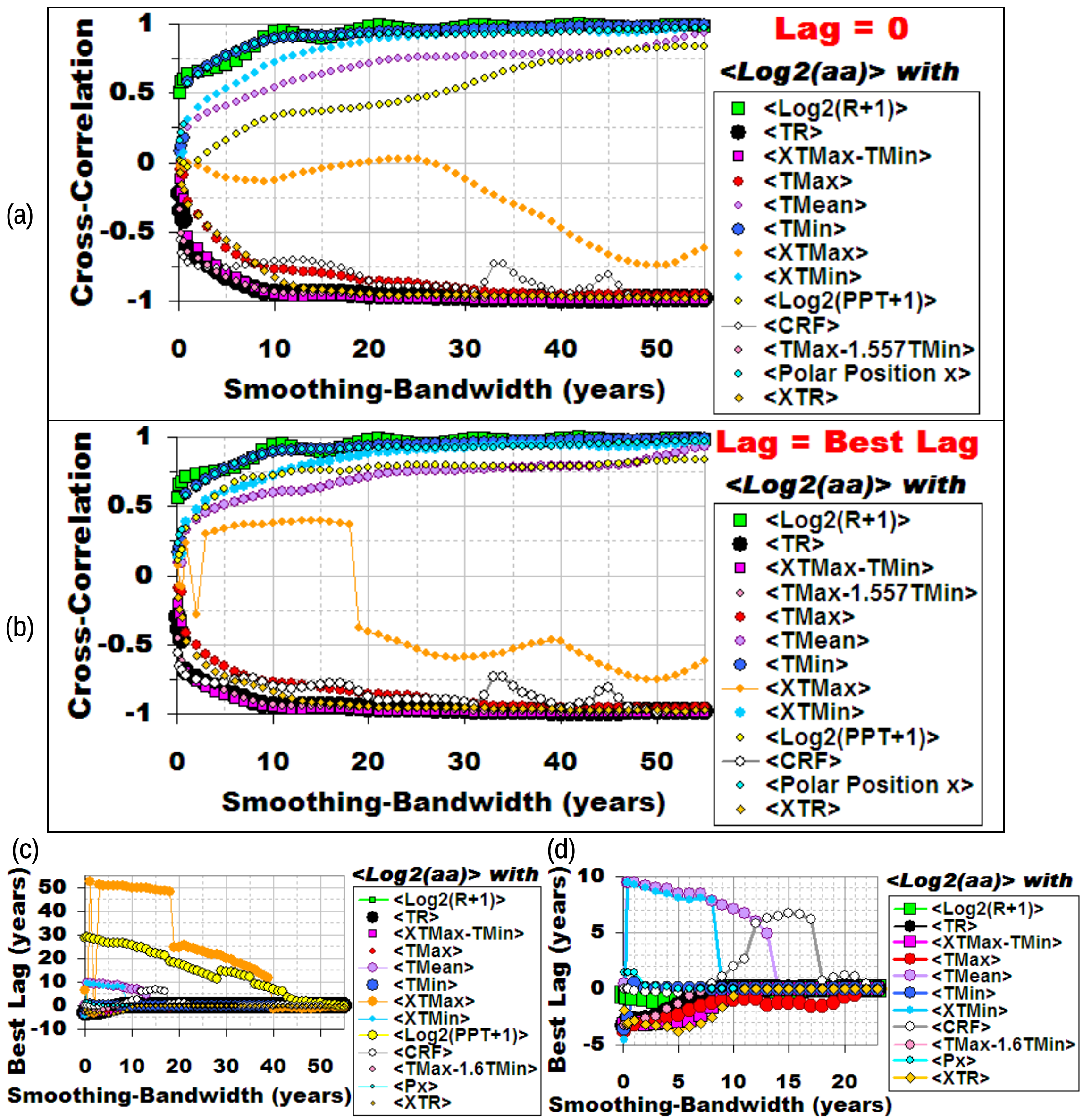

Figure 6. Summary of time-integrated cross-correlation analysis of geomagnetic aa index $\langle Log_2(aa)\rangle_w$ with a selection of study variables $\langle V\rangle_w$ (1891-2005) (where w = smoothing bandwidth in years). (a) Cross-correlations (CC) for Lag = 0. (b) Cross-correlations for Lag = Best Lag. (c) Best Lags (as judged via CC). (d) Zoom-in on Best Lags of (c).

Figure 6 provides an alternate view, expanded to include best-lags, of the relationships based on time-integrated cross-correlation. Note that the weakest relationships at lag 0 involve <PPT> & <XTMax>. These mysterious variables receive more attention below. Also worthy of note is that temperature range variables achieve best-lags of 0 by the 11a scale of time-integration, while <TMax> does not achieve a 0 best-lag until the 22a timescale. <TMin>, although weaker than temperature range variables in <aa> cross-correlations across the depicted timescale spectrum, achieves a best-lag of 0 by the 2a scale of time-integration. This is likely to be a substantial clue to anyone working on the nature of the dynamics driving the time-integrated cross-correlation patterns.

Figure 7 introduces the use of color-coded contour plots to make it possible to display time-integrated cross-correlations for a range of lags beyond just best-lags. Note that aside from some harmonic hollows related to bounded cyclical asynchrony, the time-integrated cross-correlation pattern for <aa> with <R> (Figure 6b) resembles very strongly the time-integrated auto-correlation pattern for <aa> (Figure 6a), further reinforcing points made above about the strength of the relationship between <aa> & <R>. Also note how the relationship of <aa> with <TMean> contrasts with the stronger relationships of <aa> with <TMin> and <aa> with the temperature range summary <XTMax-TMin> by noting the brighter bands near lag 0 that extend to much lower timescales for the <TMin> & <XTMax-TMin> plots than for the <TMean> plot. Finally, note the relatively anomalous appearance of the <aa> with <XTMax> plot. <XTMax> receives further attention below.

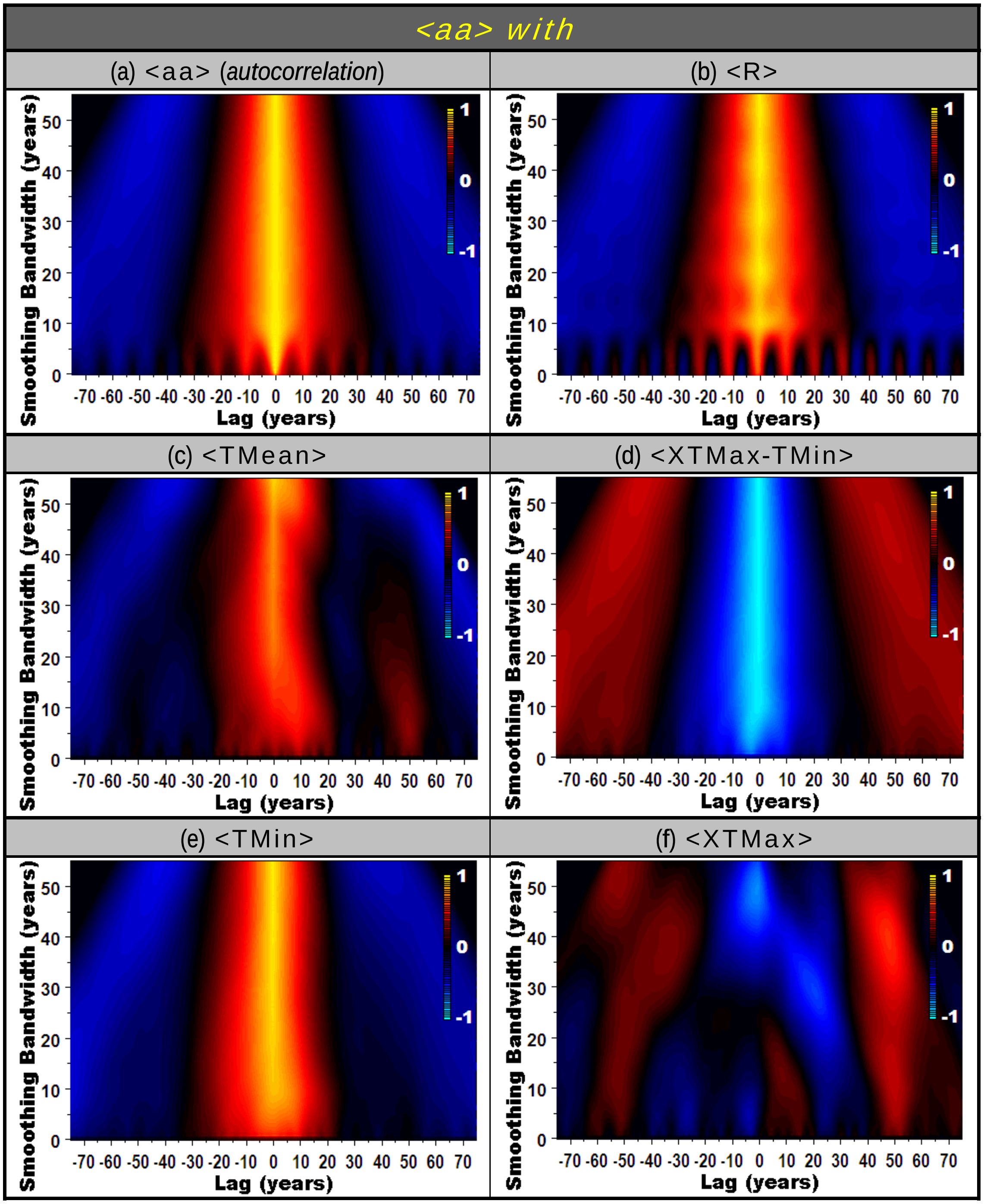

Figure 7. Time-integrated cross-correlation (1891-2005) of geomagnetic aa index <Log$_2$(aa)>$_w$ with a selection of study variables <V>$_w$ (where w = smoothing bandwidth in years). (a) <Log$_2$(aa)>$_w$ (i.e. the time-integrated autocorrelation function). (b) <Log$_2$(R+1)>$_w$. (c) <TMean>$_w$. (d) <XTMax-TMin>$_w$. (e) <TMin>$_w$. (f) <XTMax>$_w$. Note the resemblance of (a) to (b). Note that <TMin>$_w$ (e) is reliably far more strongly related to <Log$_2$(aa)>$_w$ than is <TMean>$_w$ (c) across all timescales. Also, note the way a 3-dimensional time-integrated cross-correlation plot draws attention to a loose, weak relationship; <XTMax>$_w$ (f) is seen to be only weakly related to and poorly synchronized with <Log$_2$(aa)>$_w$.

Figures 8 through 10 summarize some of the more technical details of the time-integrated relationships of <aa> with temperature variables <T>. Collectively, these figures help illustrate:

1) why the blended variable <TMean> = <(TMax+TMin)/2> exhibits weaker correlations with <aa> than do temperature range variables.
2) how time-integration over strong spectral modes adjusts the view of time-integrated relationships.

In Figure 8, two sets of cross-correlation functions are plotted in the left panel. Both involve unsmoothed (1 month timescale) temperature summaries <T>$_{\mathbf{1mo}}$, but while the first set involves unsmoothed <aa>$_{\mathbf{1mo}}$, the latter set involves 11a-smoothed <aa>$_{\mathbf{11a}}$. Focusing on the first set, note that since the signs of cross-correlations for <TMin> & <TMax> are opposite, the cross-correlations for <TMean> are muted by destructive interference while those for temperature range variables are amplified by constructive interference. Next, note that the same is true for the 11a-smoothed <aa>$_{\mathbf{11a}}$ set and also note that smoothing over the strong 11a aa spectral mode sharpens cross-correlations differentially by variable, something which is summarized for a selection of variables at intermediate levels of <aa>$_{\mathbf{w}}$ smoothing in the top right panel of Figure 8. Different temperature range characterizations are seen to capitalize on interference patterns to differing extents, but best-lags converge on 0 as the 11a <aa>$_{\mathbf{11a}}$ bandwidth is approached (Figure 8c).

It becomes evident after studying Figures 9 & 10 and then reviewing Figure 8 that <TMax-1.557TMin> is capturing seasonal information that is not captured by <XTMax-TMin> and that the relationship between <aa> and temperature variables can only be seen strongly once the strong shorter-timescale annual variation in temperature variables is sufficiently time-integrated.

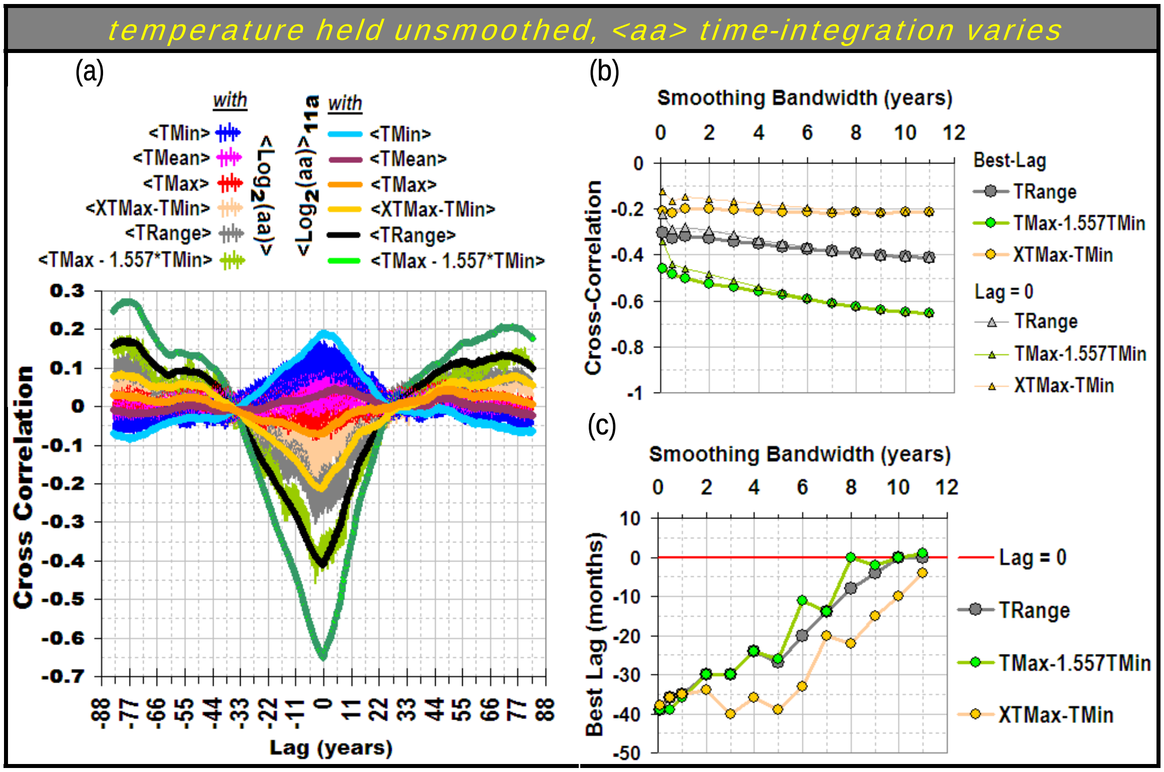

Figure 8 of . Evolution of features of the relationship between variable-smoothing-bandwidth average monthly geomagnetic aa index <Log$_2$(aa)>$_w$ (where w = smoothing bandwidth, which is 1month (i.e. unsmoothed) if not otherwise indicated) and a selection of unsmoothed Agassiz, BC average monthly temperature variables <T>$_{1mo}$ (1891-2005). (a) Cross-correlation of average monthly geomagnetic aa index <Log$_2$(aa)> and 11year-smoothed average monthly geomagnetic aa index <Log$_2$(aa)>$_{11a}$ with a selection of unsmoothed Agassiz, BC average monthly temperature variables <T>$_{1mo}$. (b) Evolution of the cross-correlation from (a) for three indicators of Agassiz average monthly diurnal temperature range, with temperature time-integration held constant at the unsmoothed 1 month timescale <T>$_{1mo}$, as the scale of aa index time-integration increases from 1mo to 11a (i.e. shifting focus from <Log$_2$(aa)>$_{1mo}$ towards <Log$_2$(aa)>$_{11a}$). (c) Evolution of the best lags associated with (b).

Figure 9 is analogous to Figure 8, with the difference being that it is <aa>$_{1mo}$ that is held unsmoothed while the degree of temperature variable time-integration varies. This provides a crude means of assessing the degree to which neglect of the dominant annual mode in the temperature series obscures the relationships between <aa> and <T>. As in Figure 8, the effects of constructive & destructive interference are seen, but in the top right panel note that the <aa>$_{1mo}$ with <T>$_w$ cross-correlation traces appear to reach the same limit with increasing time-integration. With the exception of <XTMax-TMin>$_{w}$, which involves additional high-frequency 4mo & 3mo spectral modes associated with <XTMax> that are not as thoroughly muted by smoothing as are the profiles for temperature variables with simpler spectral signatures, temperature range best-lags are seen to converge to 0 by the 11a smoothing bandwidth.

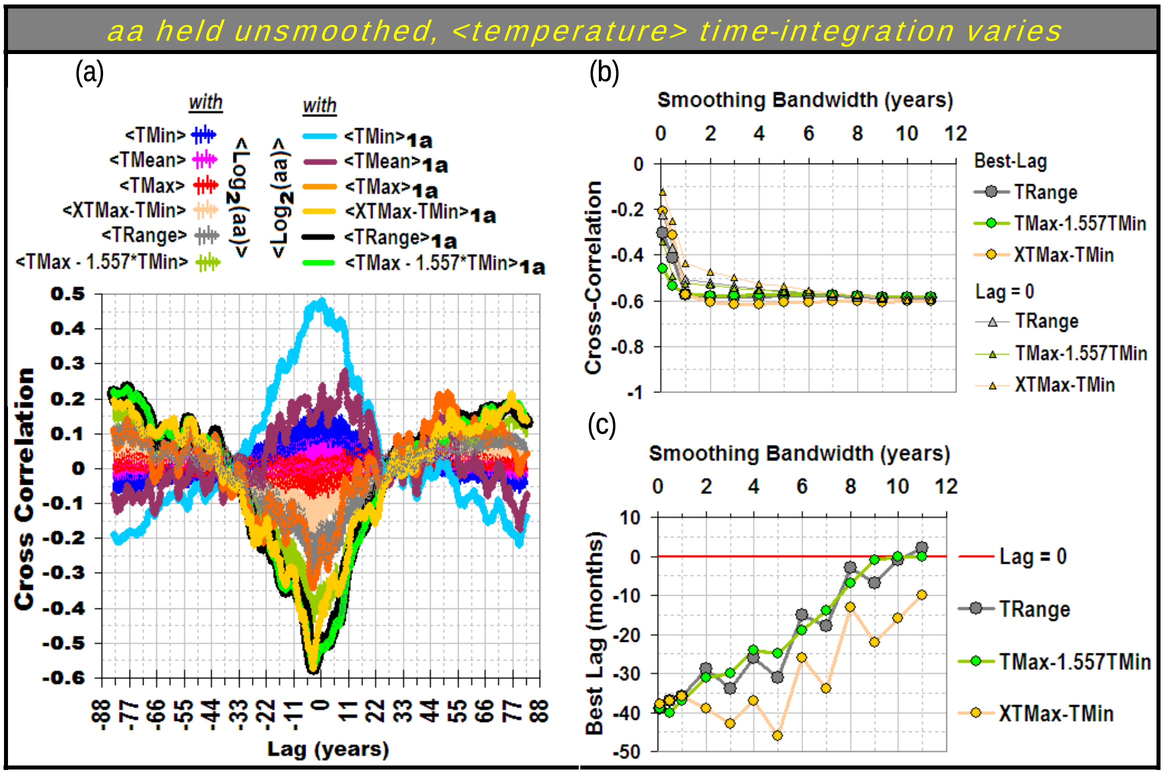

Figure 9. Evolution of features of the relationship between average monthly geomagnetic aa index <Log$_2$(aa)> and a selection of variable-smoothing-bandwidth Agassiz, BC average monthly temperature variables <T>$_w$ (1891-2005) (where w = smoothing bandwidth, which is 1month (i.e. unsmoothed) if not otherwise indicated). (a) Cross-correlation of average monthly geomagnetic aa index <Log$_2$(aa)> with a selection of unsmoothed and 11year-smoothed Agassiz, BC average monthly temperature variables, <T> & <T>$_{11a}$ respectively. (b) Evolution of the cross-correlation from (a) while <aa>$_{1mo}$ is held unsmoothed as temperature-variable time-integration is increased (i.e. shifting focus from <T>$_{1mo}$ towards <T>$_{11a}$) for three indicators of Agassiz average monthly diurnal temperature range. (c) Evolution of the best lags associated with (b).

Figure 10 includes the same reference curves in the left panel for unsmoothed <aa>$_{1mo}$ with <T>$_{1mo}$, along with cross-correlation curves for 11a smoothing of both <aa>$_{11a}$ and temperature variables <T>$_{11a}$. Note the gain in cross-correlation when time is integrated equally for both variables (left panel & top right panel). The temperature range variables are seen to juggle relative best-lag cross-correlation positions around the 1a smoothing bandwidth (top right panel), reflecting differences in the nature of their seasonal information content. It is important to keep in mind that in the right panel of Figure 10 both <aa>$_{w}$ & <T>$_{w}$ smoothing-bandwidths are being varied, whereas in each of Figures 8 & 9 one or the other of <aa> & <T> is being held unsmoothed while the degree of time-integration of the other varies. All of the presented temperature range variables achieve high cross-correlations and 0 best-lags by the 11a scale of time-integration when time is integrated equally for pairs of variables.

Although <TMin> achieves a 0 best-lag with far less time-integration (see Figure 6d), it is seen (Figure 10, left panel & Figure 6a) to retain a peak in cross-correlation of lower magnitude than those of the temperature range variables as the scale of time-integration increases. Since <TMin> is not independent of temperature range variables and since <TMax>, which is also not independent of temperature range variables, was seen above (Figure 6d) to not achieve a best-lag of 0 until the 22a scale of time-integration, it seems clear that there are some interesting dynamics at play in the <aa> relationship with temperature variables that are worthy of further study.

Partialing out time-integration information by variable, as has been done in Figures 8 to 10, helps to illustrate the breakdown of the boost in relationship detection stemming from first integrating over the lower annual mode in temperature and then continuing to integrate over the higher ~11a Schwabe mode in geomagnetic aa index. This means of exploratory investigation has the benefit of not contaminating insights with assumptions about seasonal structure that could interfere with the detection of seasonal/Schwabe interaction complexities. In a more specialized analysis, this method could be expanded to include all possible crosses of independently-varying, paired time-integration levels.

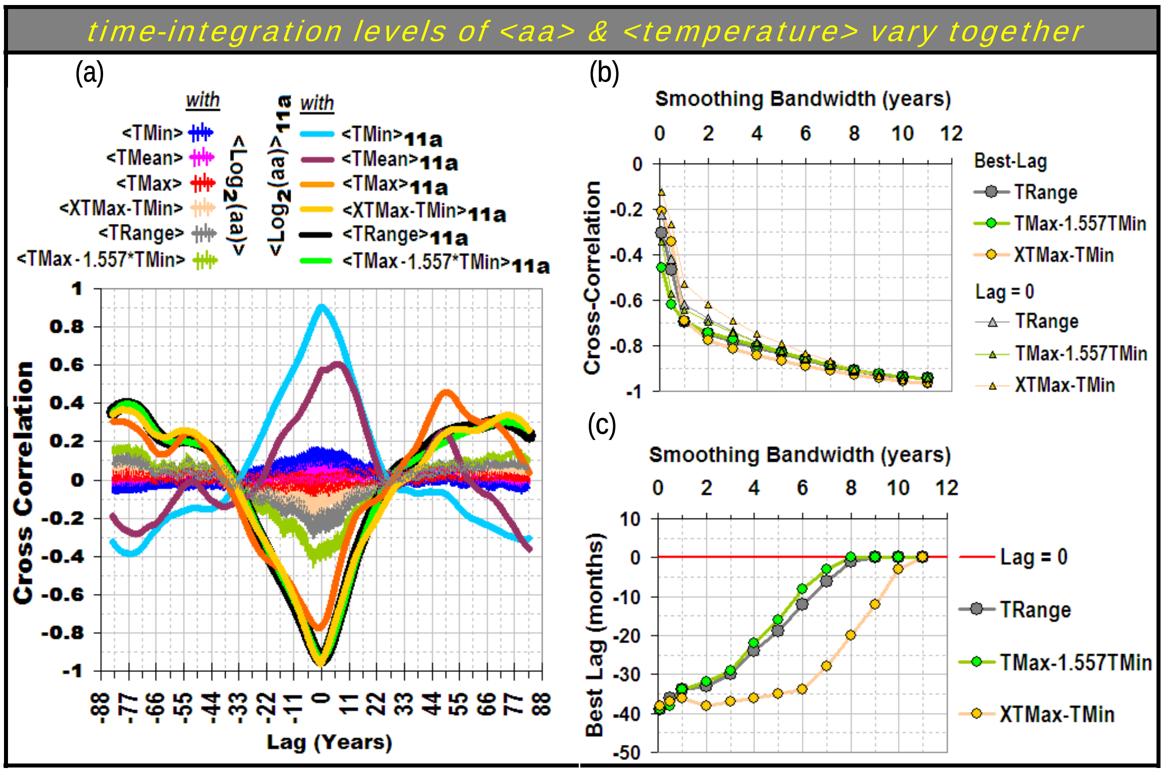

Figure 10. Evolution of features of the relationship between variable-smoothing-bandwidth average monthly geomagnetic aa index $<Log_2(aa)>_w$ (where w = smoothing bandwidth, which is 1month (i.e. unsmoothed) if not otherwise indicated) and a selection of variable-smoothing-bandwidth Agassiz, BC average monthly temperature variables $<T>_w$ (1891-2005). (a) Cross-correlation of variable-smoothing-bandwidth average monthly geomagnetic aa index $<Log_2(aa)>_w$ with variable-smoothing-bandwidth Agassiz, BC average monthly temperature variables $<T>_w$. (b) Evolution of the cross-correlation from (a) with increasing time-integration (i.e. going from $<Log_2(aa)>$ with $<T>$ to $<Log_2(aa)>_{11a}$ with $<T>_{11a}$) for three indicators of Agassiz average monthly diurnal temperature range. (c) Evolution of the best lags associated with (b).

Precipitation Relationships

The precipitation variable exhibited sufficiently distinctive patterns in its time-integrated <aa> cross-correlation relations to warrant more detailed focus. Table 4 provides a summary of the bivariate relations of <PPT> with a selection of study variables at the 11a & 22a smoothing-bandwidths. If lags of about 25 years are entertained, much stronger relationships are observed. Timescales of this size are cited by earth scientists as being important in the redistribution of water on the Earth (Vondrak 1999).

Figure 11 provides a summary of time-integrated cross-correlations for a broader selection of study variables with <PPT>, extending the view to include other scales of time-integration and reinforcing the point about roughly 25 year lags. <TMean> & <XTMax> stand out as being the weaker variables in their relationships with <PPT> across a wide range of time-integration scales. More details are shown for a selection of time-integrated <PPT> relationships in Figure 12, which provides information for lags other than best-lags, revealing a generally similar pattern shared by <R>, <aa>, <TR>, & <XTMax-TMax> in their time-integrated relations with <PPT>.

It is important to note that the results presented here are epoch-dependent. It is also worth noting that wavelet analysis reveals similar rates of <aa> & <PPT> cycling at a fairly wide range of timescales, a detail which could contribute an important focus in a more detailed future study of the complexities at work in <PPT> relations.

Table 4. Relationships of average monthly precipitation <Log_2(PPT+1)> at Agassiz, BC with a selection of study variables (1891-2005) at smoothing bandwidths of 11a & 22a.

	TMean	TMax	TMin	TRange =TMax-TMin	XTMax - TMax	Log_2(aa)	Log_2(R+1)
11 a	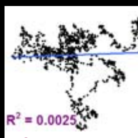 r^2 = 0.0025	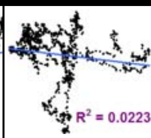 r^2 = 0.0223	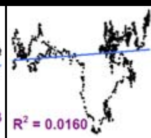 r^2 = 0.0160	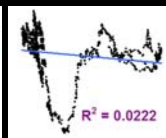 r^2 = 0.0222	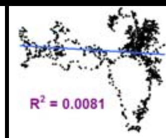 r^2 = 0.0081	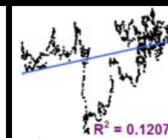 **r^2 = 0.1207**	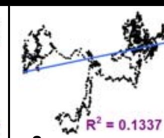 **r^2 = 0.1337**
11 a	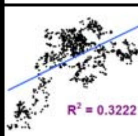 *Lag = 18a* r^2 = 0.3222	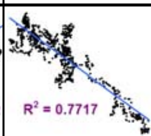 ***Lag = 25a*** **r^2 = 0.7717**	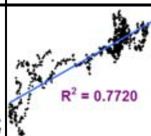 ***Lag = 24a*** **r^2 = 0.7720**	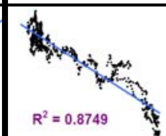 ***Lag = 25a*** **r^2 = 0.8749**	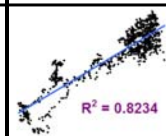 ***Lag = 24a*** **r^2 = 0.8234**	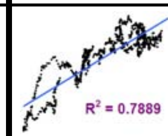 ***Lag = 25a*** **r^2 = 0.7889**	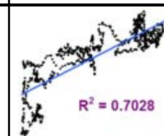 ***Lag = 25a*** r^2 = 0.7028
22 a	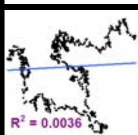 r^2 = 0.0036	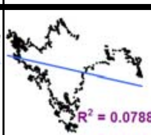 r^2 = 0.0788	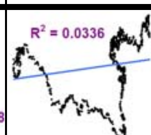 r^2 = 0.0336	 r^2 = 0.0518	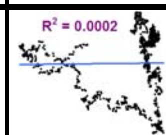 r^2 = 0.0002	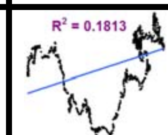 **r^2 = 0.1813**	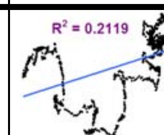 r^2 = 0.2119
22 a	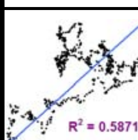 *Lag = 16a* r^2 = 0.5871	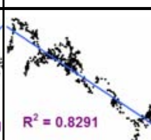 ***Lag = 25a*** **r^2 = 0.8291**	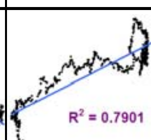 ***Lag = 25a*** **r^2 = 0.7901**	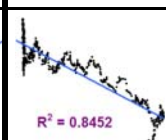 ***Lag = 25a*** **r^2 = 0.8452**	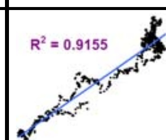 ***Lag = 24a*** r^2 =0.9155	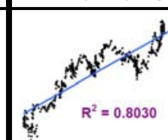 ***Lag = 26a*** **r^2 = 0.8030**	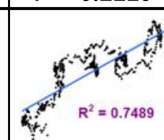 ***Lag = 26a*** r^2 = 0.7489

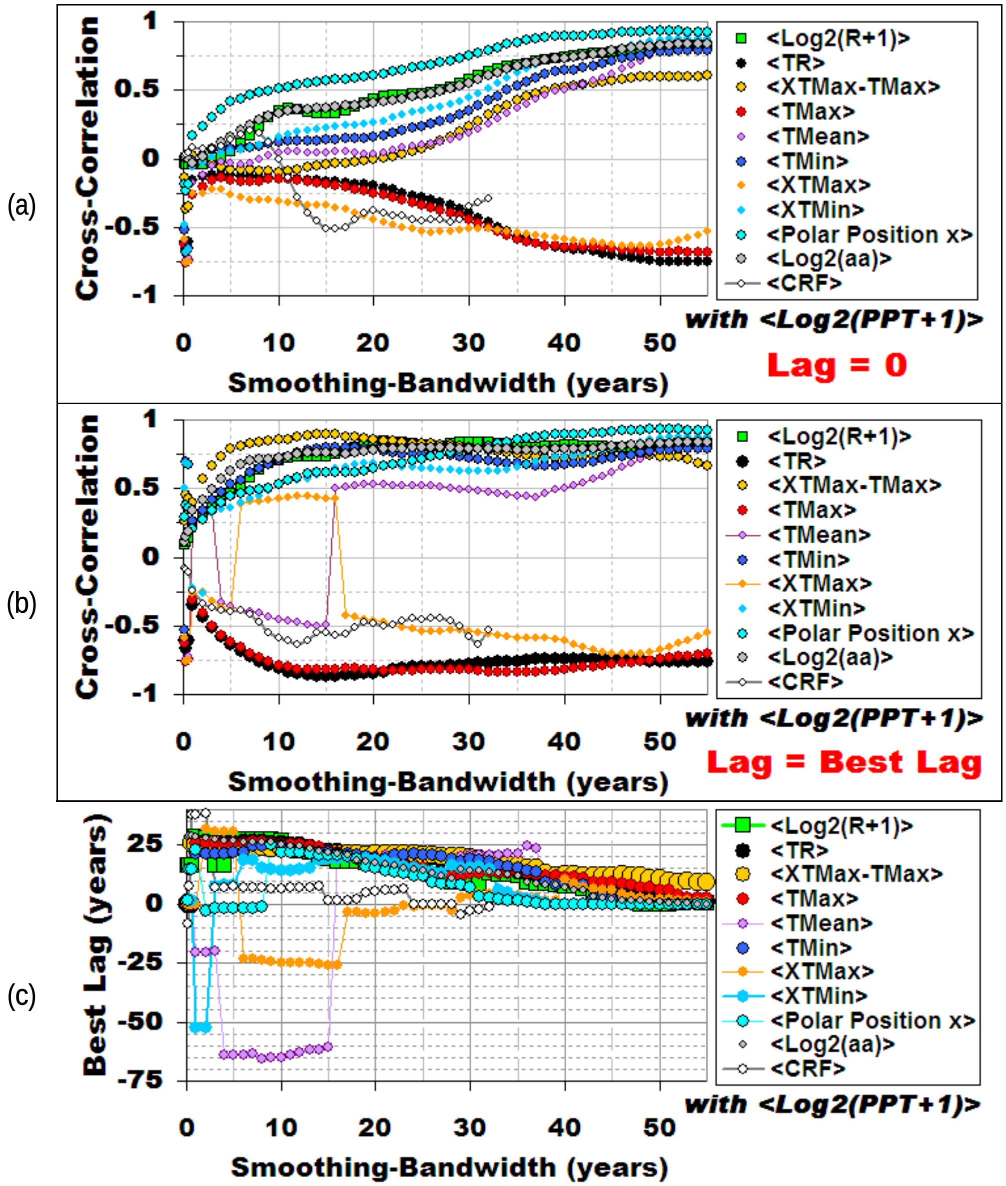

Figure 11. Summary of time-integrated cross-correlation analysis (1891-2005) for a selection of study variables <V>$_w$ with Agassiz, BC average monthly precipitation <Log$_2$(PPT+1)>$_w$ (where w = smoothing bandwidth in years). (a) Cross-correlations for Lag = 0. (b) Cross-correlations for Lag = Best Lag. (c) Best Lags. Note the heavy concentration of variables with a <Log$_2$(PPT+1)>$_{1mo}$ best-lag of ~26a.

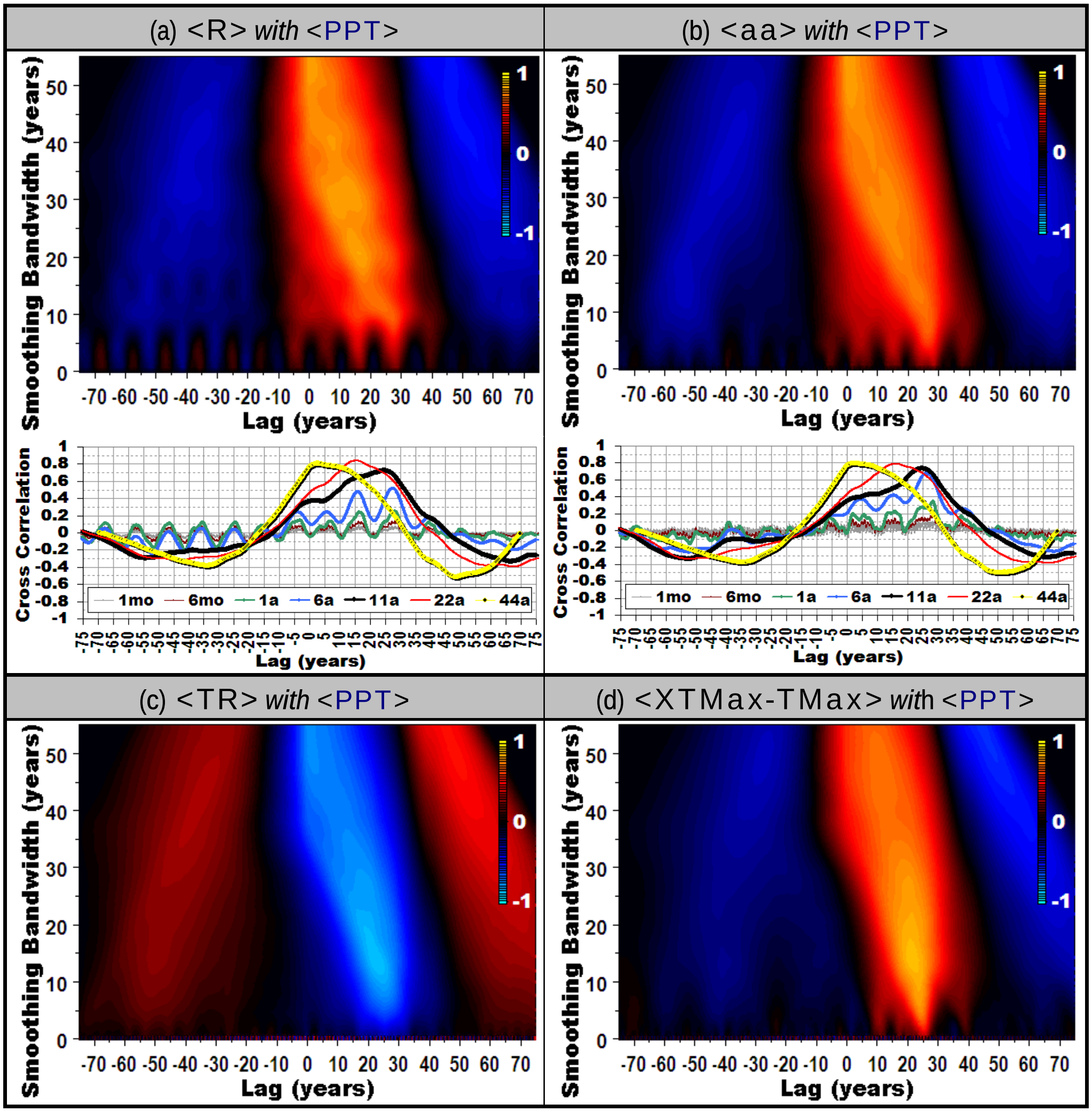

Figure 12. Time-integrated cross-correlation (1891-2005) of (a) sunspot number <Log_2(R+1)>$_w$ (with traditional-style plot illustrating specified horizontal-slices beneath to assist viewers who are unaccustomed to reading color-contour plots) (b) geomagnetic aa index <Log_2(aa)>$_w$ (with traditional-style plot beneath), (c) <TRange>$_w$, and (d) <XTMax-TMax>$_w$ with Agassiz, BC average monthly precipitation <$Log_2$2(PPT+1)>$_w$ (where w = smoothing bandwidth). Precipitation at Agassiz, BC shows complex epoch-dependent relationships with other study variables.

Relationships Involving Extreme Maximum Monthly Temperature, Cosmic Ray Flux, & Solar Inertial Motion

The relatively complex time-integrated relationships of <XTMax> (Figures 13 & 14a,b,&c) led to the inclusion of cosmic ray flux <CRF> as a study variable. <CRF> is strongly cyclically synchronized with both <R> & <aa>, as summarized in Figure 15, but the timescale-dependent features of <CRF> relationships with <R> & <aa> reflect substantial complexity.

(a)

(b)

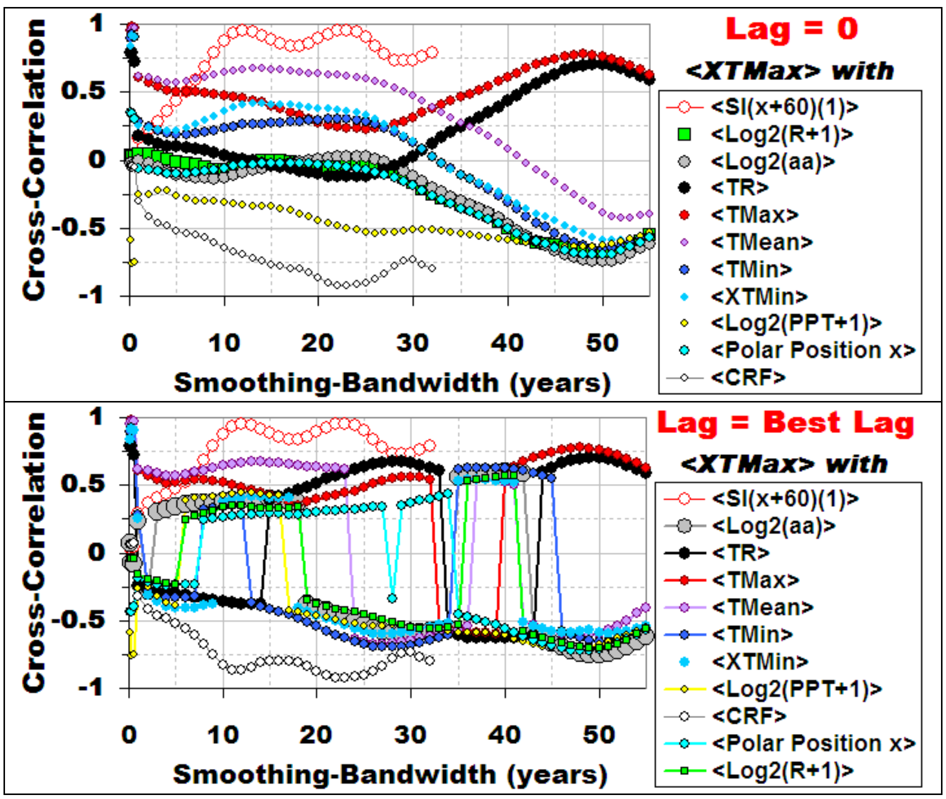

Figure 13. Summary of time-integrated cross-correlation analysis of monthly extreme temperature range <XTMax>$_w$ with a selection of study variables <V>$_w$ (where w = smoothing bandwidth in years). (a) Cross-correlations for Lag = 0. (b) Cross-correlations for Lag = Best Lag. *The <SI$_{x+60°}$(1)> and <CRF> series depicted here only cover 1953-2005. All other series depicted here cover 1891-2005.*

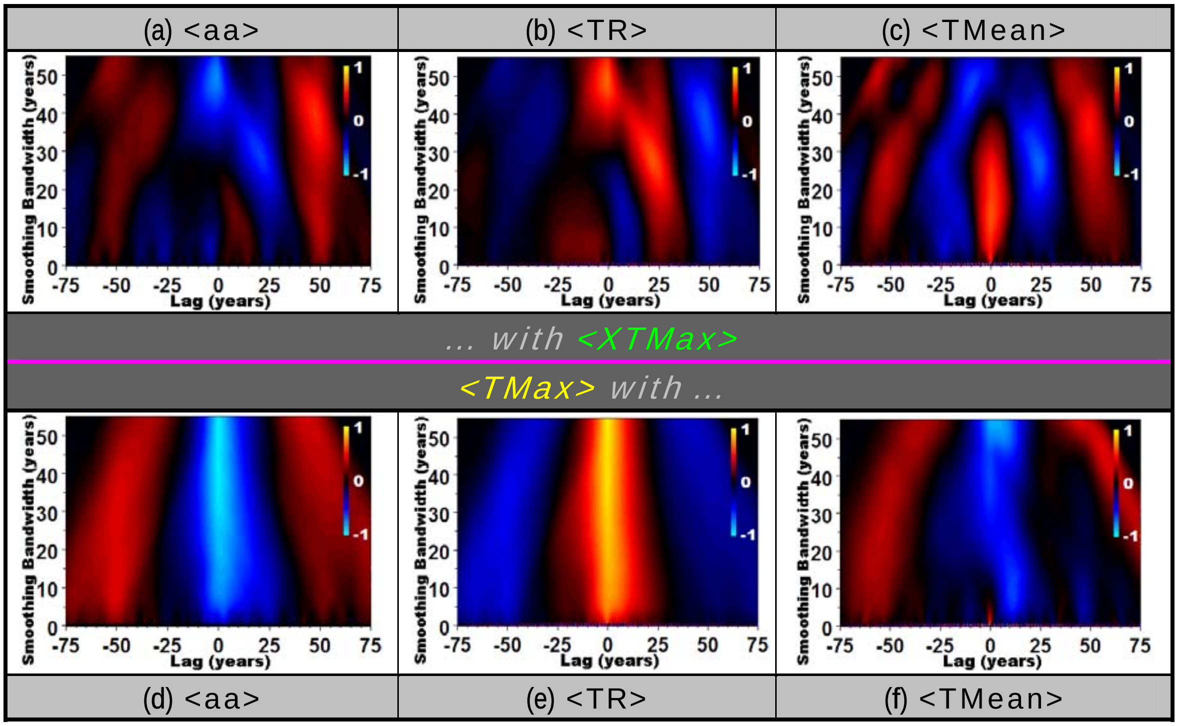

Figure 14. Time-integrated cross-correlation (1891-2005) of (a) geomagnetic aa index <Log$_2$(aa)>$_w$, (b) <TR>$_w$, and (c) <TMean>$_w$ with Agassiz, BC extreme maximum monthly temperature <XTMax>$_w$ (where w = smoothing bandwidth). For comparison: Time-integrated cross-correlation (1891-2005) of <TMax>$_w$ with (d) geomagnetic aa index <Log$_2$(aa)>$_w$, (e) <TR>$_w$, and (f) <TMean>$_w$, (where w = smoothing bandwidth). <XTMax> at Agassiz, BC shows complex epoch-dependent relationships with other study variables. The vertical bands in these plots at ~25a & ~50a are suggestive of statistical resonance modes.

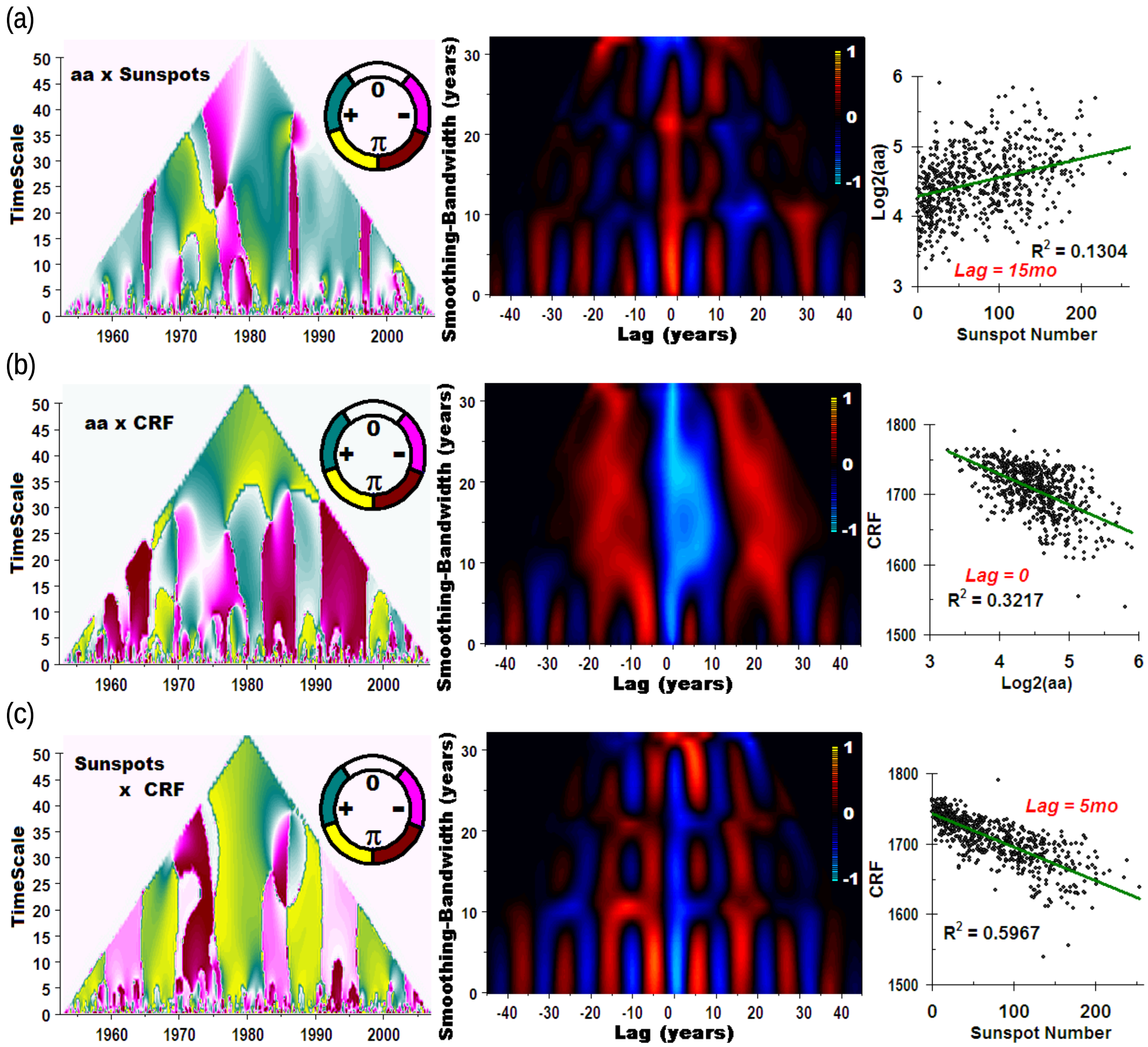

Figure 15. Cross-wavelet transform phase-difference, time-integrated cross-correlation, and monthly-timescale best-lag scatterplots for pairs of solar activity-related indices (1953-2005). (a) Geomagnetic aa index <Log$_2$(aa)> with cosmic ray flux <CRF>. (b) Geomagnetic aa index <Log$_2$(aa)> with sunspot number <Log$_2$(R+1)>. (c) Sunspot number <Log$_2$(R+1)> with cosmic ray flux <CRF>.

Regardless of the level of our present understanding, we can start by mapping out the morphology of relations. In the present study, a strong relationship is found to exist, during the epoch for which <CRF> data is available (1953-2005), between <CRF> & <XTMax> at the 11a & 22a year timescales, the timescales of the solar Schwabe & Hale cycles (Figures 13b & 16). During the limited record interval, <CRF> exhibits an even-odd pattern alternation that is related to the solar polarity reversal about midway through each ~22a magnetic Hale cycle (Figure 1). In light of this, stronger 0 lag cross-correlations & tighter best-lags around the 22a timescale, relative to those around the 11a timescale, are not surprising (Figures 13 & 17a). <TMax> relates nearly as strongly to <CRF> as does <XTMax>, but it is important to be aware that <TMax> shows relatively less enigmatic time-integrated relations with other study variables than does <XTMax> (Figure 14).

Both <XTMax> & <CRF> exhibit strong time-integrated relations with patterns of solar motion about the barycentre of the solar system over the interval for which <CRF> data is available (Figures 13, 16, & 17). When considering the apparent 1953-2005 epoch Schwabe/Hale-timescale 3-way relationship involving <XTMax>, <CRF>, & <SI>, it is worth keeping in mind that the latter half of the 20th century contrasts with the earlier half in the following ways: (1) rapidly rising atmospheric CO_2 concentrations; (2) high average geomagnetic activity; (3) low temperature ranges; (4) regular 9 year tidal-event period (versus 6 year period in the early 20th century) (Keeling & Whorf 1997); and (5) "slightly disordered" (1957-2005) solar inertial motion pattern (versus "trefoil, stable" pattern 1906-1956) (Charvatova 2007). These &/or other factors may play important roles in modulating dominances over & between epochs. Further investigation will be necessary to further characterize &/or rule out the apparent relationships.

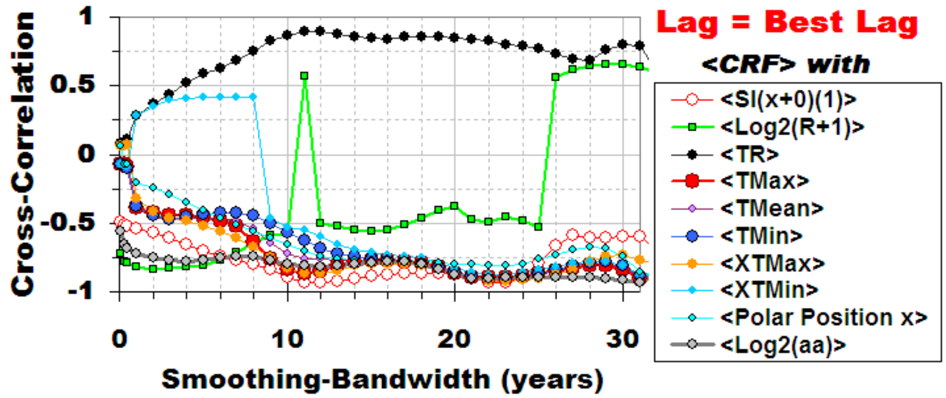

Figure 16. Time-integrated cross-correlations (Lag = Best Lag; 1953-2005) for cosmic ray flux <CRF>$_w$ with a selection of study variables <V>$_w$ (where w = smoothing bandwidth in years).

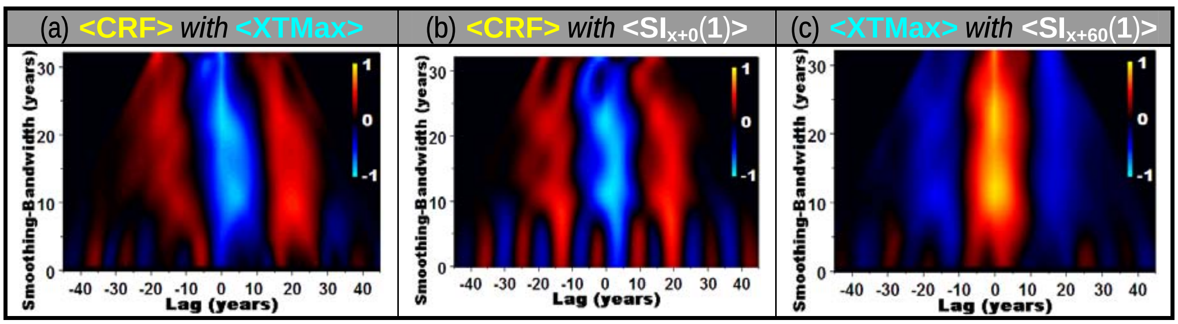

Figure 17. Time-integrated cross-correlation (1953-2005) of cosmic ray flux <CRF>$_w$ with (a) <XTMax>$_w$ and (b) <SIM$_{x+0°}$(1)>$_w$, (where w = smoothing bandwidth). (c) Time-integrated cross-correlation (1953-2005) of extreme monthly maximum temperature at Agassiz, BC <XTMax>$_w$ with <SI$_{x+60°}$(1)>$_w$.

As a final note, Figure 17c draws attention to a relationship involving a 60° rotation. In order to explore anisotropy, the coordinate frame of solar motion was rotated to investigate how time-integrated cross-correlation patterns vary with spatial-orientation. During the present study, it was found that some orbital/rotational relationships, including the (apparent) ones involving solar motion with <XTMax> & <CRF>, exhibit considerable anisotropy and that while negative best-lags might appear at some reference frame orientations, positive best-lags can appear at others, providing a means of investigating any lags that are puzzling in light of imaginable causation-chains.

Polar Position

It has been suggested that terrestrial polar position is an indicator of the lunar nodal cycle and that it is related to Arctic temperature series (Yndestad 2006). Leaving aside the issue of whether polar position is primarily conveying information about the lunar nodal cycle, polar position was investigated for time-integrated cross-correlations with a selection of study variables. Rotations of the polar position coordinate axes were also explored to assess the influence of spatial orientation on relationships. It was determined that orientation has an effect on the nature of the relationships observed, but further details on orientation are omitted because the original polar position x & y orientations provide nearly optimal orientations for the purposes of the present research.

Summaries of time-integrated relationships involving polar position x direction are presented in Figure 18. Figure 19 includes additional detail for a smaller selection of the relationships. Polar position shows strong relationships with <aa>, <TMin>, & temperature range variables. It shows a weaker relationship with <TMean> and an even weaker relationship with <XTMax>. Studies that focus solely on the relationships between mean temperatures and polar position might benefit from a broadening to include additional summaries.

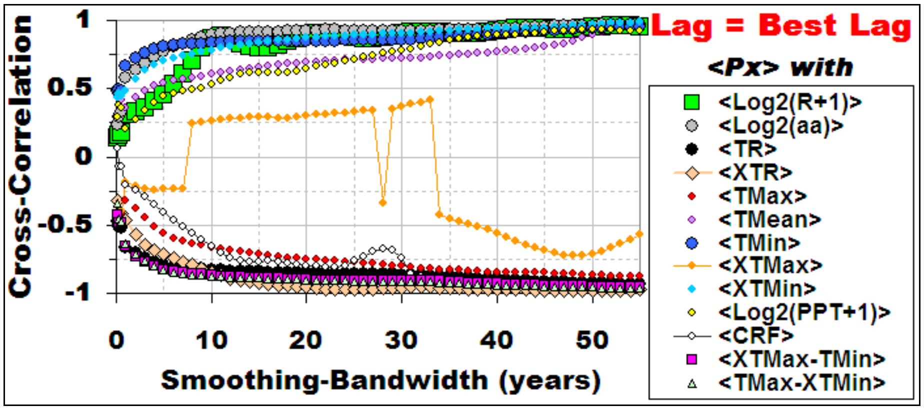

Figure 18. Time-integrated cross-correlations (Lag = Best Lag; 1891-2005) for polar position x-direction $<P_x>_w$ with a selection of study variables $<V>_w$ (where w = smoothing bandwidth in years). While a lot of studies in the literature focus on mean temperature variables, this summary suggests that investigating alternative summaries may be fruitful.

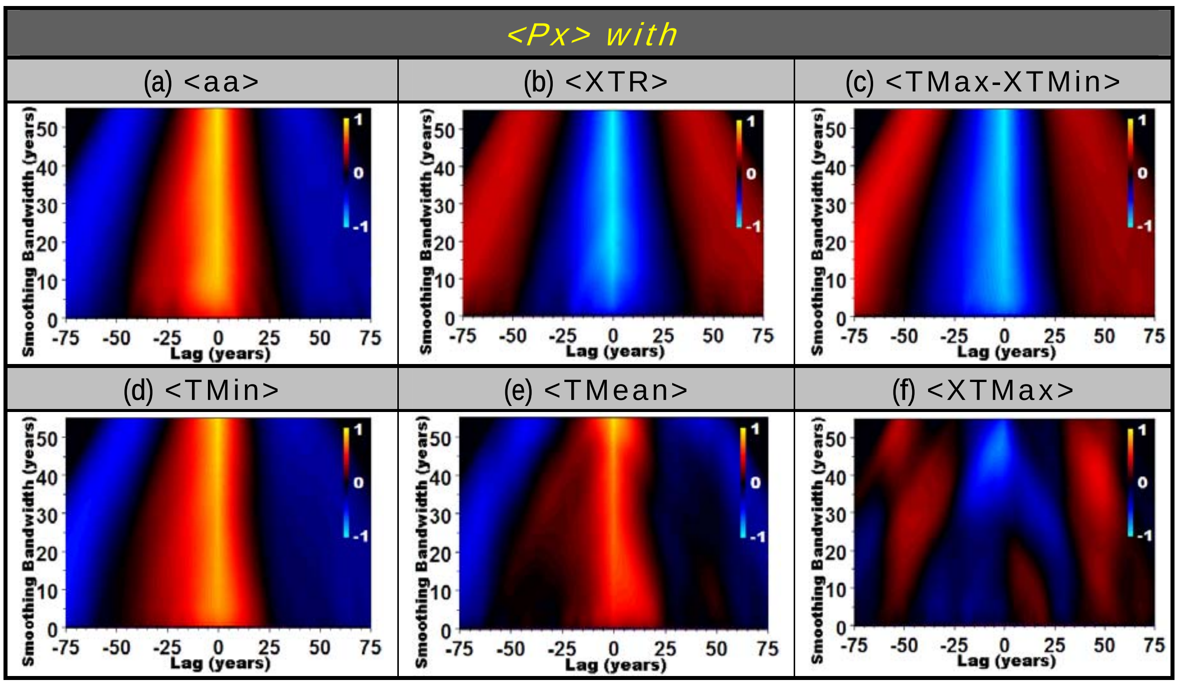

Figure 19. Time-integrated cross-correlation (1891-2005) of polar position x-direction $<P_x>_w$ with (a) geomagnetic aa index $<Log_2(aa)>_w$ and Agassiz, BC average monthly temperature range indices (b) $<XTR>_w = <XTMax-XTMin>_w$, (c) $<TMax-XTMin>_w$, (d) $<TMin>_w$, (e) $<TMean>_w$, and (f) $<XTMax>_w$, (where w = smoothing bandwidth).

Alternate Characterizations of Solar System Orbital Inertia, with Focus on Possible Relationships with Polar Position

A class of solar system orbital inertia (SI(k)) characterizations, in which jovian planet contributions are weighted by fractional moments mr^k, $k \in$Real, was investigated for relationships with a selection of other study variables. Jose (1965) presented a few examples of SI characterizations and stressed that any number of other characterizations are possible. Orbital angular momentum (OAM) is one SI characterization which has received considerable attention in the literature (Landscheidt 1999; Jakubcova 1985; Wilson et al. 2009; Juckett 2000). OAM can easily be derived from the class of SI characterizations investigated in the study at hand.

A number of Landscheidt's publications (1998-2002) focused on variation of OAM at particular timescales, such as 3 years and 9 years. Variable time-integration was introduced in the present study to expand the view across a spectrum of timescales. Landscheidt found very interesting correlations, but skeptics appear to have suspended judgement for now, possibly awaiting concrete documentation on physical mechanisms. The variable moment-degree in the present study was initially introduced to help sharpen the perception of fundamental SI oscillations (which were found to be muted around 1930, for example, in the OAM series), but it proved to also produce provocative correlations, some of which are worthy of report even in the present absence of full theoretical support. Also noteworthy, attentiveness to spatial orientation has led to an enhanced awareness of nearly-neighboring timescale modes that could easily be overlooked by investigators. Juckett (2000) appears to have arrived at a similar insight.

The lissajous pattern of the relative jovian planet orbits results in an epitrochoid orbit of the sun around the solar system barycentre (Figure 20). Color-contour plots of time-integrated SI time series and their spatial orientation vector-decompositions, along with a selection of derivatives, draws visual attention to striking periodicities (that can be confirmed spectrally) that exhibit correspondingly striking time-integration properties.

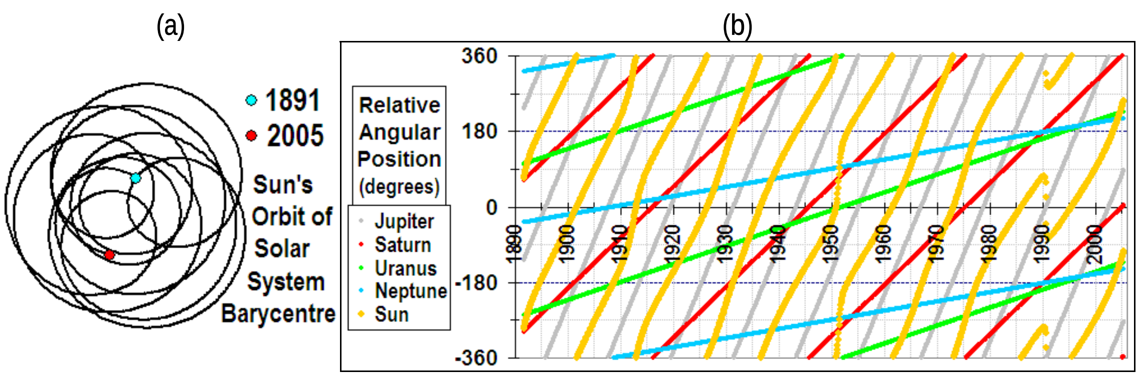

Figure 20. (a) Sun's orbit of solar system barycentre (1891-2005). (b) Relative angular position (°) of the Sun & the four Jovian planets, Jupiter (J), Saturn (S), Uranus (U), & Neptune (N) (1891-2005).

The first inertial moment, SI(1), with planet contributions weighted by mr^1, is a scalar multiple of the variable-radius of the sun's orbit, so it can be interpreted as characterizing the sun's physical position relative to the solar system barycentre. Not surprisingly, due to Jupiter's mass and the modulation of its influence by its most frequently encountered and most massive neighbor Saturn, a roughly 19.76a cycle is prominent in this series, with an alternating intensity on odd cycles induced by lower frequency beats between the gas giants. However, investigating derivatives of SI characterization, via differencing, increasingly reveals (Figure 21 a-c (top row)) a seemingly fundamental half-period of about 6.4a (over the interval 1891-2005), which falls just below the third harmonic of the Jupiter-Saturn (JS) synodic period and very close to the half-period of the Jupiter-Neptune (JN) synodic period.

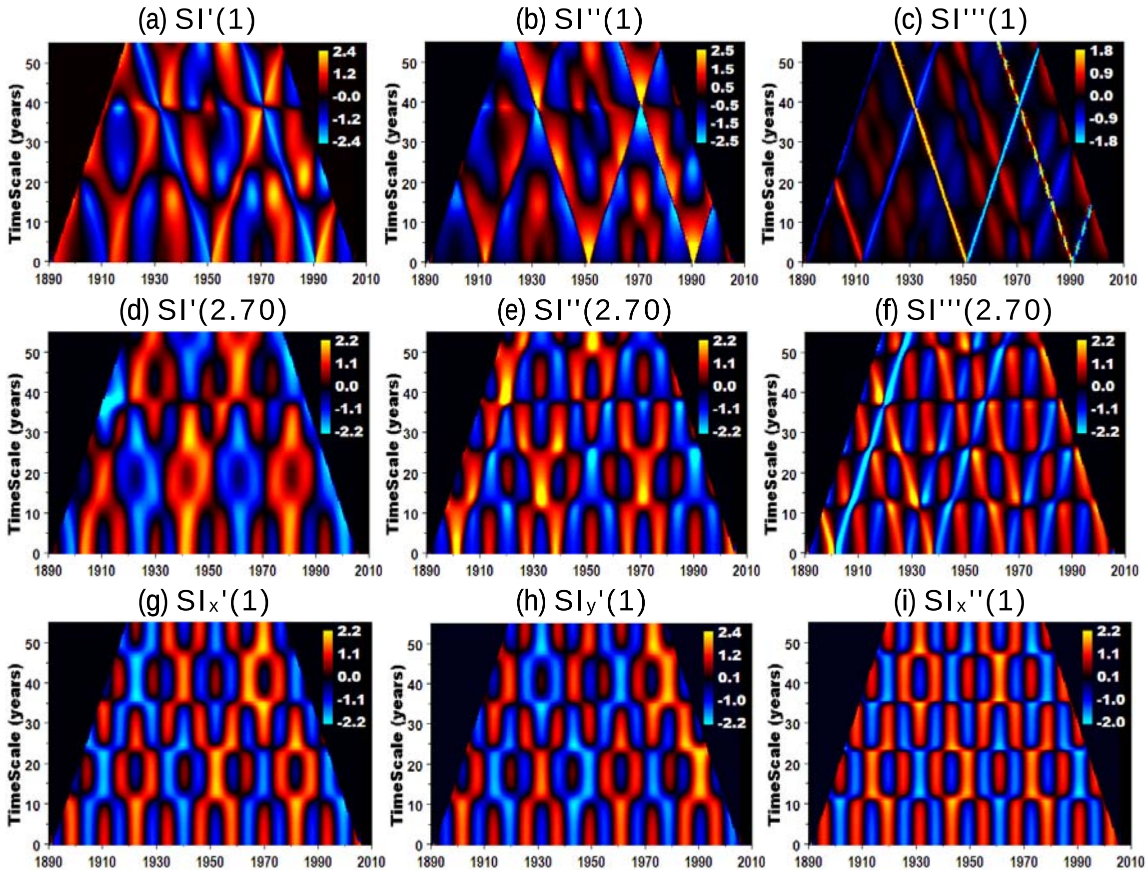

Figure 21. Standardized time-integrated time series (1891-2005): (a) SI'(1). (b) SI''(1). (c) SI'''(1). (d) SI'(2.70). (e) SI''(2.70). (f) SI'''(2.70). (g) $SI_x'(1)$. (h) $SI_y'(1)$. (i) $SI_x''(1)$. The 1st through 3rd derivative fractional k=2.70a moment of inertia SI sequence adjusts non-linear distortions to sharpen the view of the ~6.4a beat half-period. (Compare d-f with a-c.) Also, note the slight downshift in period for the axial series (g-i).

To see this better, the time-smoothed spectrum of the SI characterization for a fractional moment of k=2.70, SI(2.70), chosen to equalize the relative influence of Saturn & Uranus, is presented (Figure 21 d-f (middle row)). This emphasizes the ~6.4a alternation, particularly with increasing derivatives. Harmonics & subharmonics (confirmed spectrally) show up visually with time-integration. These harmonics & subharmonics coincide with a pattern of lags found in solar-terrestrial-climate relations in the present study.

When polar SI characterizations are re-expressed as axial components, $SI_x(k)$ & $SI_y(k)$ in a Cartesian spatial frame, which is easily rotated to further explore the possible significance of orientation, for example due to field anisotropies, a slightly downshifted harmonic spectrum of important timescales is revealed (Figure 21 g-i (bottom row)), as is to be expected due to the dominant high-frequency content due to Jupiter's orbit (1/11.85a).

At this point, considering the properties of terrestrial polar position wave structure in more detail is constructive (Figure 22).

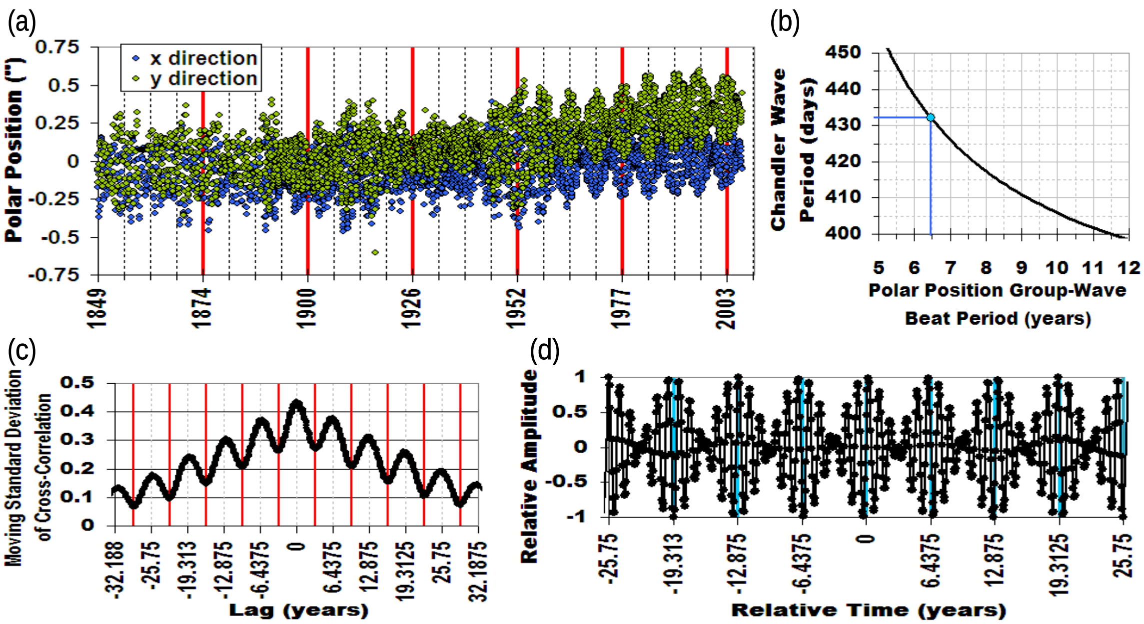

Figure 22. (a) Polar position motion (deviation from a standard reference in arcseconds(")) during the interval 1849-2007. The lower density of dots at the left end of the plot is due to the half-as-frequent measurements before 1890. The horizontal grid-spacing of the plot draws attention to features of the group wave structure. Note the apparent phase-shift somewhere near 1930. (b) Resonance curve depicting the theoretical acoustic relationship between polar position group-wave & the terrestrial Chandler period. (c) 3 year moving standard deviation of the cross-correlation of polar position x direction with polar position y direction. This highlights the group-wave period of ~6.4a to ~6.5a. (d) Group-wave structure manufactured using acoustic theory to demonstrate the interference (via superposition) of an annual sinusoidal wave and the resonance of that annual wave with a sinusoidal wave that has a period of 6.4375a.

The period of ~6.4a, which seems to be a feature shared by SI & polar motion structure, prompted a new line of investigation, the very earliest results of which are summarized in Figure 23, which reveals a relationship involving a striking phase concordance (after 1935) & rough anti-concordance (before 1920) on either side of a transitional interval centred near 1930, which is roughly coincident with a similar time-window given special attention by Vondrak (1999) due to a phase-reversal of Earth's Chandler wave over this interval. Ongoing investigation of this provocative relationship, although at a preliminary stage, is yielding insights which are consistent with the early insights presented here.

A period of about 6.4a has shown up many times in the present study. 6.4 years is, for example, roughly:

1) a multiple or factor of many of the best-lags discovered via even a very crude initial time-integrated-relationship exploration. See Figure 1b.
2) the fourth harmonic of the best-lag for the time-integrated cross-correlation function of several study variables with <PPT>. For example, at the 11a timescale, for <aa>$_{\mathbf{11a}}$: 25.75a / 4. See the bright bands angling down towards ~26a in Figure 12, Figure 11c, & the bottom row of Table 4.
3) the fourth & eighth harmonics of the best-lags, at noteworthy timescales, for the time-integrated cross-correlation function of several study variables with <XTMax>. For example, at the 11a timescale, for <aa>$_{\mathbf{11a}}$: 51.5a / 8. See the bright bands over ~25a & ~50a in Figure 14a,b,&c and also see <XTMax> in Figure 6c.

(a)

(b)

(c)

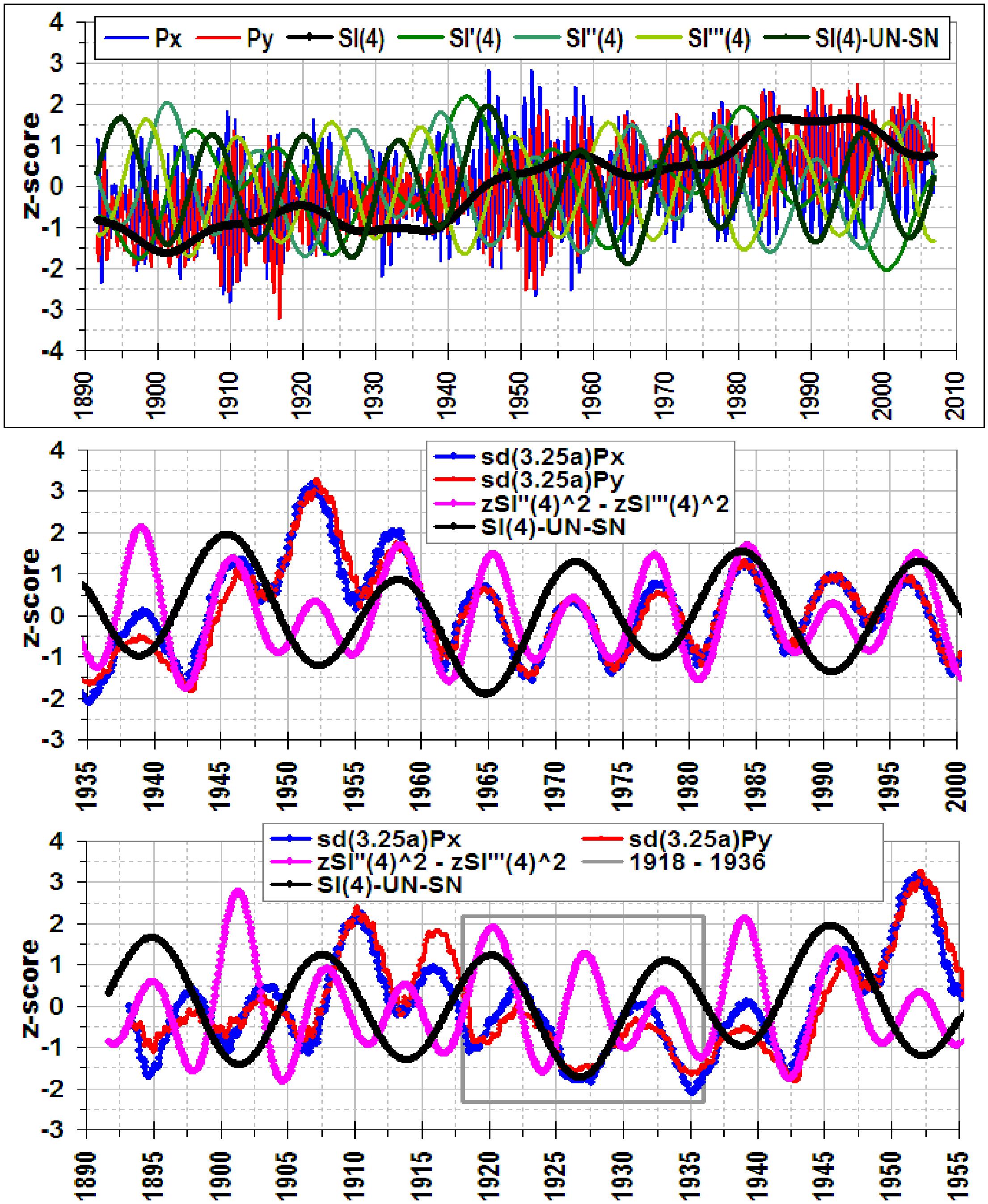

Figure 23. Standardized (a) polar position & $SI^n(4)$ derivative series for n=0,1,2,3 (1891-2005) and 3.25a-moving-standard-deviation of P_x & P_y along with the function ${}_zSI''(4)^2$ - ${}_zSI'''(4)^2$ for the intervals (b) 1935-2000 & (c) 1890-1955, drawing attention a striking phase concordance (after 1935) & rough anti-concordance (before 1920) on either side of a transitional interval centred near 1930, which is roughly coincident with a similar time-window given special attention by Vondrak (1999) due to a phase-reversal of Earth's Chandler wave over this interval. The SI(4) curve with low-frequency Uranus-Neptune (UN) & Saturn-Neptune (SN) influences removed is included on plots as an alternate means of drawing attention to the ~6.4a timing of beats.

4) twice the best-lag for the cross-correlation of Agassiz, BC monthly average diurnal temperature range with monthly geomagnetic aa index (unsmoothed). See first row of Table 3, Figure 6d, & Figure 10c.

5) the best-lag (or a harmonic thereof) for a variety of other relationships investigated during the course of this study, for example several involving solar system orbital inertial characterizations. For one example, see <XTR> in Figure 24d.

6) the period of the polar position group wave, the resonance period of the Earth's Chandler wobble with the Earth's annual wobble, & the oscillatory period of the 3-year moving standard deviation of the auto- & cross-correlation functions for all possible crosses of P_x & P_y (confirmed spectrally). See Figures 22 & 23.

7) the seemingly fundamental mode (confirmed spectrally) that shows up in the harmonic spectrum of a variety of characterizations of solar system orbital inertia, which, upon very detailed preliminary investigation, seems to fall roughly between the 25th (6.59a) & 26th (6.34a) harmonics of the orbital period of Neptune (164.79a). See Figures 21 & 23.

8) the resonance period of pairs of roughly annual-to-biennial timescale solar periodicities, which seem related, on average perhaps, over epochs, according to the acoustic identity BP(T/k,T/(k+1)) = T (where BP denotes beat period) with T = ~6.4a in the present case. For example: BP(3.2a,2.13a), BP(2.13a,1.6a), & BP(1.6a,1.28a). (Relevant references: Mursula et al. 2003, 2004, & 1999; Javaraiah 2003; Charvatova 2007; Kato et al. 2003; Krivova & Solanki 2002).

It is worth noting that Yndestad (2006) interprets periodicities such as 25a, 50a, & 75a as being related to lunar nodal harmonics. Insights stemming from the present study raise the issue of possible confounding. Gross' findings (2005) regarding polar motion leave questions regarding the drivers of the atmospheric & oceanic pressures and Landscheidt (1999) did find correlations between solar OAM and the terrestrial southern oscillation index, which is based on atmospheric pressures over the ocean & related to global climate patterns. Disentangling possibly-shared harmonics, possibly stemming from mutual influences, will require further investigation.

Finally, the results of time-integrated cross-correlation analyses involving <SI(4)> are summarized in Figures 24-26. <SI(4)> appears to be strongly related to <P_y> and to also be relatively strongly related to <aa> & <XTR> across a wide range of timescales over the interval 1891-2005. Analogous to what has been reported with respect to relationships explored above, <TMin> exhibits a tight lag pattern and <TMean> is considerably weaker than <TMin> in its <SI(4)> relationship, while <XTMax> is even weaker. A picture of a seemingly-related group of variables is emerging. It is worth noting that <SI_y(4)> exhibits exceptionally high time-integrated cross-correlations with <P_y> above the 1a timescale, along with a striking 0 best-lag at all timescales (Figure 26).

Some of the strong relationships found may be coincidental, but while they do not necessarily reflect real physical linkages, further investigation, along at least some of the lines introduced & explored above, seems warranted.

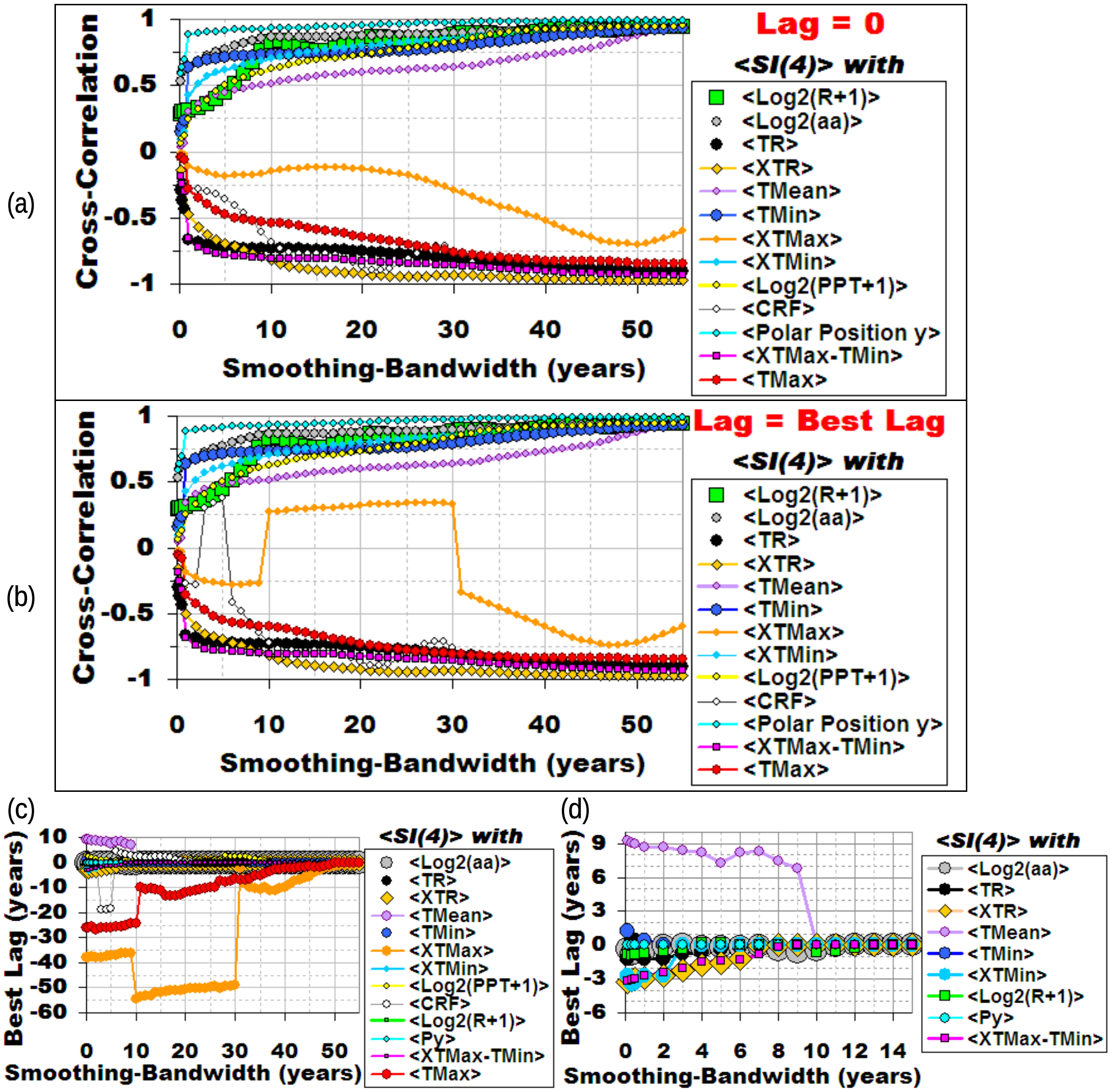

Figure 24. Time-integrated cross-correlation analysis (1891-2005) summary for a fourth-moment solar system jovian-planet orbital inertia characterization <SI(4)>$_w$ with a selection of study variables <V>$_w$ (where w = smoothing bandwidth in years).

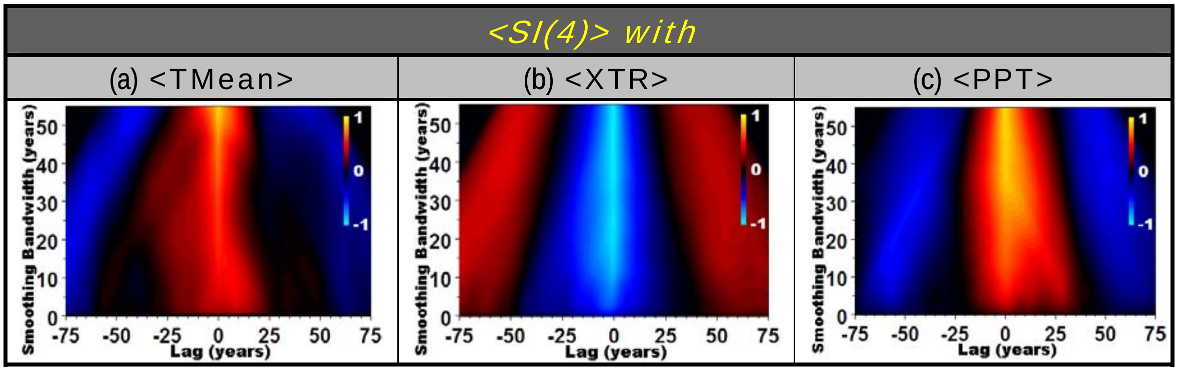

Figure 25. Time-integrated cross-correlation (1891-2005) of <SI(4)>$_w$ with Agassiz, BC (a) average monthly temperature <TMean>$_w$, (b) monthly extreme temperature range <XTR>$_w$ = <XTMax-XTMin>$_w$, and (c) average monthly precipitation <Log$_2$(PPT+1)>$_w$, (where w = smoothing bandwidth).

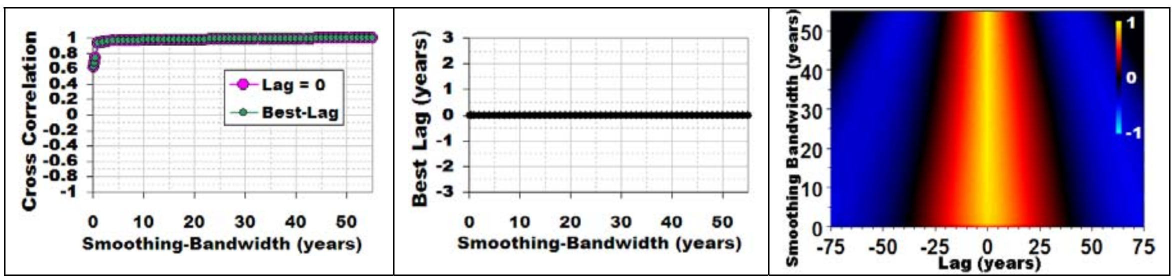

Figure 26. Time-integrated cross-correlation analysis (1891-2005) summary for <SI$_y$(4)>$_w$ with <P$_y$>$_w$, (where w = smoothing bandwidth).

Atmospheric CO_2

The strongest time-integrated cross-correlations found for <CO_2> (Figure 27) give cause for a cautionary note. Any monotone time series with a short record length (Figure 28) is susceptible to exhibiting high correlations with any other time series that are non-undulating over the short era. The weakest time-integrated cross-correlations with <CO_2> (1958-2005) were for study time series that oscillate, such as sunspot number <R>. Even the sunspot number envelope oscillates during the period for which modern <CO_2> measurements are available; hence the lower time-integrated cross-correlations with <CO_2> in comparison with, for example, <CRF>, another fairly sharply oscillating series, which shows a strengthening in its relationship with <CO_2> at the 22a timescale as oscillations associated with the Hale solar cycle are smoothed over.

The strong time-integrated relationship between <CO_2> & the polar position y-direction and the exceptionally strong time-integrated relationship between <CO_2> & the y-direction of the fifth-moment solar system orbital inertia characterization <$SI_y(5)$>, while interesting, may indicate nothing about physical linkages. For the purposes of the present study, no strong conclusions are being drawn regarding <CO_2>, but it does appear reasonable to suggest that minimum temperatures at Agassiz, BC are more strongly related to & more tightly synchronized with <CO_2> than are maximum temperatures at sub-Hale timescales.

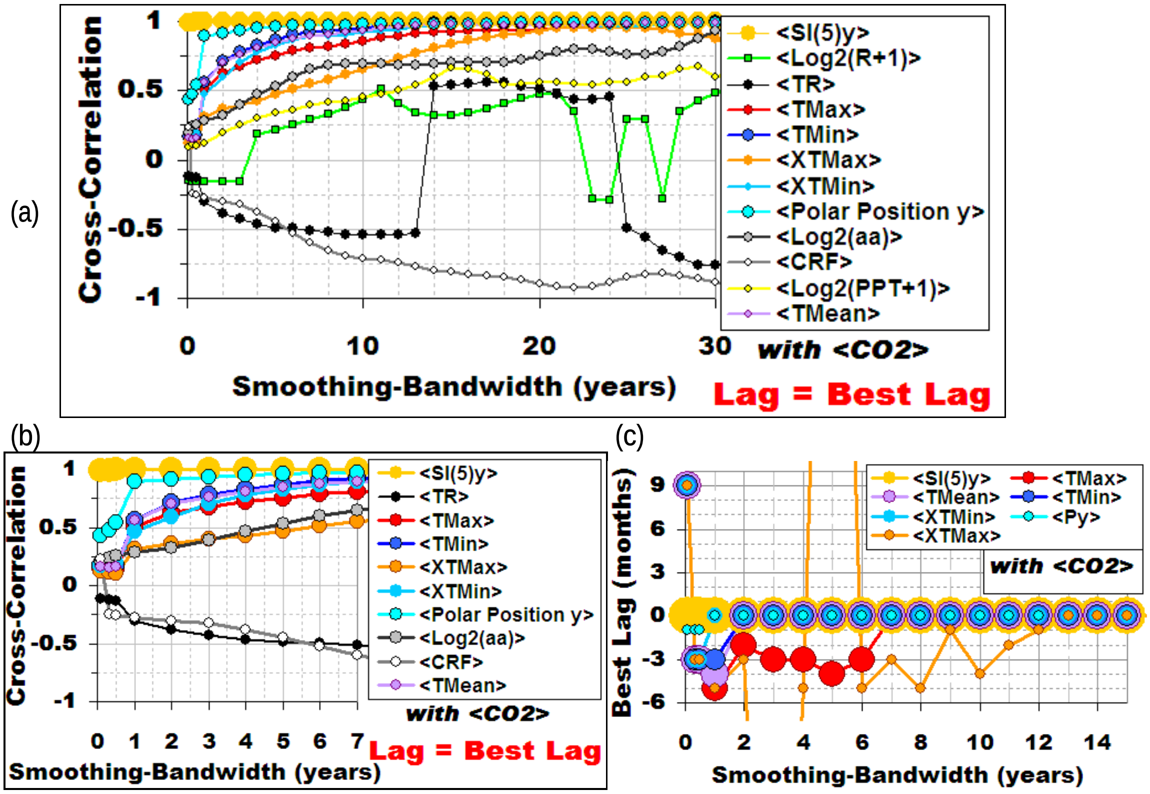

Figure 27. Summary of time-integrated cross-correlation analysis (1958-2005) for a selection of study variables $<V>_w$ with atmospheric carbon dioxide concentration $<CO_2>_w$ (where w = smoothing bandwidth in years). (a) Cross-correlations for Lag = Best Lag. (b) Focus on lower timescales & a subset of variables from (a). (c) Best Lags (in months). Minimum temperature summaries appear more strongly related to & more tightly synchronized with $<CO_2>_w$ than are their maximum temperature analogs at sub-Hale timescales. $<P_y>_w$ appears more strongly related to $<CO_2>_w$ than is $<TMin>_w$, but this may be coincidental. The high $<CO_2>_w$ correlation with $<CRF>_w$ centred at the 22a timescale is worthy of note and $<XTMax>_w$ peaks in its relationship with $<CO_2>_w$ at around the same timescale. By far the most striking feature of this group of plots is the cross-correlation of over 0.99 between $<CO_2>_w$ & $<SI_y(5)>_w$ across all timescales right down to the grain (1 month), with a best-lag of 0 across the board; however, this strong coincidence may reflect absolutely nothing about physical linkages (see text).

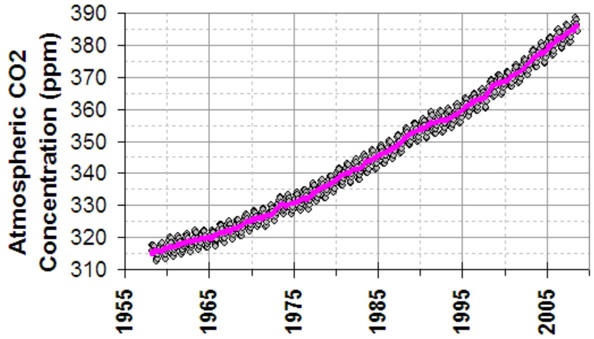

Figure 28. Monthly atmospheric CO_2 concentration at Mauna Loa (1958-2008) with annual average superimposed.

Conclusions

Temperature patterns at Agassiz, BC over the interval 1891-2005 show a relationship with geomagnetic aa index at the timescale of the solar Schwabe (~11a) cycle. A few of the highlights are as follow:

1) Indices of average monthly temperature range, which can be expressed as differences or as ratios of absolute temperatures, are the temperature variables that show the strongest time-integrated relationship with geomagnetic aa index across all investigated timescales.
2) Average monthly minimum temperature shows the tightest lag pattern in its time-integrated relationship with geomagnetic aa index.

Terrestrial polar motion, indices of solar system orbital inertia, & geomagnetic aa index are more strongly related to average monthly temperature ranges & minima at Agassiz, BC over the interval 1891-2005 than to means across all investigated timescales.

Terrestrial polar motion shows a very strong time-integrated relationship with an index of solar system orbital inertia over the interval 1891-2005 across all super-annual timescales and, more generally, further investigation may be warranted in light of a variety of striking features of relationships involving solar system orbital inertia and terrestrial polar motion, including seemingly-related non-random best-lag patterns which appear in the time-integrated relationships of Agassiz, BC monthly weather summaries.

Further investigation may also be warranted with regards to the following noteworthy findings:

1) Atmospheric carbon dioxide concentrations appear to have a stronger time-integrated relationship with Agassiz, BC average minimum monthly

temperatures than with average monthly maximum temperatures at sub-Hale timescales over the study interval for which carbon dioxide data is available, 1958-2005.

2) Average monthly precipitation at Agassiz, BC shows a time-integrated relationship with geomagnetic aa index over the interval 1891-2005 if lags of about 25 years are entertained.

3) Agassiz, BC extreme maximum monthly temperature shows a strong time-integrated relationship with both cosmic ray flux and an indicator of solar system orbital inertia over the study interval for which cosmic ray flux data is available, 1953-2005, at both the solar Schwabe (~11a) & Hale (~22a) timescales.

Closing Remarks

Improvements to climate models depend in part upon deepening understanding of complex natural climate variation. Even if some of the findings of the present study are ephemeral, epoch-dependent, &/or site-specific, they may provide important clues about solar-terrestrial-climate harmonics and dynamics more generally.

BIBLIOGRAPHY

Abarca del Rio, D., Gambis, D., Salstein, P., Nelson & Dai, A. (2003). Solar activity and earth rotation variability. *Journal of GeodynamicS, 36,* 423–443.

Alania, M. V., Gil, A., & Modzelewska, R. (2008). 27-day variations of the galactic cosmic ray intensity and anisotropy. *Astrophys. Space Sci. Trans., 4,* 31–34.

Alexander, W. J. R., Bailey, F., Bredenkamp, D. B., van der Merwe, A. & Willemse, N. (2007). Linkages between solar activity, climate predictability and water resource development. *Journal of the South African Institution of Civil Engineering, Vol 49 No 2,* 32–44, Paper 659.

Allen, T.F.H. & Hoekstra, T. W. (1992). *Toward a unified ecology*. New York: Columbia University Press.

Allen, T. F. H. & Hoekstra, T. W. (1991). *Role of heterogeneity in scaling of ecological systems under analysis.* In: Ecological Heterogeneity. Kolasa, J. & Pickett, S. eds. Springer Verlag, New York. 47-68.

Allen, T. F. H. (1987). Hierarchical complexity in ecology: a noneuclidean conception of the data space. *Vegetatio 69:* 17-25.

Babcock, H.W. (1961). The topology of the Sun's magnetic field and the 22-yr cycle. *Astrophysical Journal, 133,* 572-587.

Baliunas, S. L., Lockwood, G. W., Skiff, B.A. & Radick, R. R. (1992). Long-term brightness changes estimated from a survey of Sun-like stars *solar. Nature.*

Baliunas, S. & Soon, W. (1995): Are variations in the length of the activity cycle related to changes in brightness in solar-type stars? *Astrophysics* Journal. 450 (1995), 896.

Brunetti, M. Buffoni, L., Maugeri, M. & Nanni, T. (2000). *Trends of Minimum and Maximum Daily Temperatures in Italy from 1865 to 1996.* Theor. Appl. Climatol. 66, 49±60 Brzezinski, A. (2003). Oceanic Excitation of Polar Motion and Nutation: An Overview. *IERS Technical Note No. 30.*

Brzezinski, A. (2003). Oceanic Excitation of Polar Motion and Nutation: An Overview. *IERS Technical Note No. 30.*

Bucha, V., Jakubcov´a, I., & Pick, M. (1985). Resonance frequencies in the Sun’s motion, *Studia Geophys. et Geod*., 29, 107–111.

Cadavid, A. C., Lawrence, J. K., McDonald, D. P. & Ruzmaikin, A. (2005). *Independent Global Modes of Solar Magnetic Field Fluctuations*. Kluwer Academic Publishers.

Canadian Council of Ministers of the Environment. (2003). Climate, Natue, People: Indicators of Canada's Changing Climate.

Casdagli, M. (1991). Chaos and Deterministic versus Stochastic Non-Linear Modelling *Journal of the Royal Statistical Society. Series B (Methodological*), Vol. 54, No. 2, 303-328.

Cayan, D. R., (1996). Interannual climate variability and snowpack in the western United States. *Journal of Climate*, 9, 928-948.

Celaya, M. A., Wahr, J. M. & Bryan, F. O. (1999). Climate-driven polar motion. *Journal of Geophysical Research, Volume 104, Issue B6*, 12813-12830.

Cerveny, R. S., and J. A. Shaffer (2001). “The Moon and El Niño.” *Geophysical Research Letters*, 28(1), 25–28.

Chao, B. F., Au, A. Y. (2002). Amalgamation of the North Atlantic Oscillation and North Pacific Oscillation into an Annular Mode. American Geophysical Union, Spring Meeting 2002. 05/2002.

Chapanov, Ya. (2005). On the long-periodical oscillations of the earth rotation. Available online at: http://syrte.obspm.fr/journees2005/s2_12_Chapanov.pdf

Chapanov, Ya., Vondrak, J. & Ron, C. (2007). Decadal Oscillations of The Earth Rotation. Available online at: http://pecny.asu.cas.cz/cedr/download/chapanov1a.pdf

Chapanov, Ya., Gambis, D. (2007). Correlation between the solar activity cycles and the earth rotation. Available online at: http://syrte.obspm.fr/journees2007/PDF/s4_18_Chapanov.pdf

Charvátová, I. (2009). Long-term predictive assessments of solar and geomagnetic activities made on the basis of the close similarity between the solar inertial motions in the intervals 1840–1905 and 1980–2045. *New Astronomy, 14*, 25–30.

Charvátová, I., Ivanka, I., Jaroslav & Strestik. (2007). Relations between the solar inertial motion, solar activity and geomagnetic index aa since the year 1844. *Advances in Space Research, 40,* 1026–1031.

Charvátová, I. (2007). The prominent 1.6-year periodicity in solar motion due to the inner planets. *Ann. Geophys., 25,* 1227–1232.

Charvátová, I. (2000). Can origin of the 2400-year cycle of solar activity be caused by solar inertial motion? *Ann. Geophysicae 18,* 399-405.

Charvatova, I. & Strestik, J. (2004). Periodicities between 6 and 16 years in surface air temperature in possible relation to solar inertial motion" Journal of Atmospheric and Solar-Terrestrial. *Physics* 66 (2004) pp219-227.

Cliver E.W. & A.G. Ling (2002). Secular change in geomagnetic indices and the solar open magnetic flux during the first half of the twentieth century *J.Geophys Res*, 107, A10.

Cliver, E. W. & Boriakoff, V. (1996). The 22-year cycle of geomagnetic and solar wind activity. *Journal Of Geophysical Research, Vol. 101, No. A12,* 27091-27109.

Cliver, E. W., Boriakoff, V. & Feynman, J. (1998). Solar variability and climate change: Geomagnetic aa index and global surface temperature. *Geophysical Research Letters*, *Vol. 25, No. 7,* p.1035-1038.

Currie, R. G. (1996). Variance contribution of luni-solar (Mn) and solar cycle (Sc) signals to climate data. *International Journal of Climatology, Vol. 16, No. 12,* 1343-1364.

Damon & Laut. (2004). Pattern of Strange Errors Plagues Solar Activity and Terrestrial *Climate Data*, *vol. 85, No. 39*, 370-374.

Damon, P. E. & Peristykh, A. N. (2003). Persistence of the Gleissberg 88-year solar cycle over the last ~12,000years: Evidence from cosmogenic isotopes. *Journal Of Geophysical Research, Vol. 108, No. A1, 1003*, 2003.

Da Silva, R. R., Avissar, R. (2005). The impacts of the Luni-Solar oscillation on the Arctic oscillation. *Geophys. Res. Lett.,* 32, L22703. Available at http://cat.inist.fr/?aModele=afficheN&cpsidt=17380045

David, A. (2007). *The Past and Future of Climate.* Lavoisier Conference, Melbourne.

Dudok, T., de Wit. (2005). *Did the solar open magnetic field really double in one century?* (LPCE, Orléans). COST Action 724 Athens, 12 October 2005.

Delcourt P., & Delcourt, H. (1991). *Quaternary ecology: A paleoecological perspective.* N.Y: Springer.

Del Río, S., Fraile, R., Herrero, L. & Penas, A. (2007). Analysis of recent trends in mean maximum and minimum temperatures in a region of the NW of Spain (Castilla y León). *Theoretical and Applied Climatology, Volume 90, Numbers 1-2,* 1-12.

Dewey, E. R. (1970). *Cycles; selected writings*. Pittsburgh: Foundation for the Study of Cycles.

Djurovic, D. & Paquet, P. (1999). Some fresh indications of the solar origin of 4-6-year oscillation of the earth's rotation parameters. *Serbian Astronomical Journal, 159,* 1-10.

Djurovic, D. & Paquet, P. (1996). The common oscillations of solar activity, the geomagnetic field, and the Earth's rotation. *Solar Physics, 167,* 427-439.

Duhau S. & Chen, C. Y. (2002). The sudden increase of solar and geomagnetic activity after 1923 as a manifestation of a non-linear solar dynamo. *Geophysical research letters*, *vol. 29, no 3*, 6.1-6.4.

Easterling, D. R., Briony, H., Jones, J. P. D., Peterson, T.C., Karl, T. R., Parker, D. E., et al. (1997). Maximum & Minimum Temperature Trends for the Globe. *Science, New Series, Vol. 277, No. 532,* 364-367.

Echer-Souza, M. P., Echer, E., Rigozo, N. R. & Nordemann, D. J. R. (2006). On the dependence of global surface air temperature on solar and geomagnetic activity. *Geophysical Research Abstracts, Vol. 8, 00318. European Geosciences Union 2006.*

Eddy, J. A.. The Maunder Minimum. *Science,* 192, 1189-1202. The volume number is included: 192.

Fairbridge, R. W. (2002). Climate and Keplerian Planetary Dynamics: The "Solar Jerk", The King-Hele Cycle, and the Challenge to Climate Science. *21st Century Science and Technology.* Available online at: http://www.crawfordperspectives.com/Fairbridge-ClimateandKeplerianPlanetaryDynamics.htm

Fairbridge, R. W., Hillaire-Marcel, C. (1977). An 8,000-yr palaeoclimatic record of the 'Double-Hale' 45-yr solar cycle. *Nature, 268,* 413 – 416. (04 Aug 1977).

Feynman, J. $ Ruzmaikin, A. (1999). Modulation of cosmic ray precipitation related to climate. Geophysical Research Letters*,* 26 (14): 2057-2060 JUL 15 1999

Fichtner, Horst, Scherer, Klaus; Heber, Bernd. (2008). Solar or cosmic ray forcing of the terrestrial climate? 37th COSPAR Scientific Assembly. Held 13-20 July 2008, in Montréal, Canada., p.881.

Fichtner, H., Scherer, K. & Heber, B. (2006)**.** A criterion to discriminate between solar and cosmic ray forcing of the terrestrial climate. *Atmos. Chem. Phys. Discuss., 6,* 10811–10836.

Fodor, I. K. & Kamath, C. (n.d.). Using independent component analysis to separate signals in climate data. Available online at https://computation.llnl.gov/casc/sapphire/pubs/151808.pdf

Forster, P. M. De F., and S. Solomon, 2003. Observations of a "weekend effect" in diurnal temperature range. Proc. Natl. Acad. Sci. U. S. A., 100, 11225–11230. Available online at:

http://homepages.see.leeds.ac.uk/~earpmf/papers/ForsterandSolomon2003.pdf

Fotheringham, A. S. & Rogerson, P. A. (1993). "GIS and Spatial Analytical Problems", *International Journal of Geographic Information Systems, Vol., 7, No. 1,* 3-19.

Foukal, D., Fröhlich, C., Spruit, H. & Wigley. T.\M.L.(2006). Nature 443, 161-166 (14 September 2006). Available online at: http://www.nature.com/nature/journal/v443/n7108/full/nature05072.html

Freeman, J. C. & Hasling, J. F. (2004). *An orbital motion shared by sun and earth effecting sunspots and earth weather.* Available online at: http://www.wxresearch.org/papers/orbit2004.htm

Friis-Christensen, E. & Lassen, K. (1991). Length of the solar cycle: An indicator of solar activity closely associated with climate. *Science, 254,* 698-700.

Gedalof, Z.; & Smith, D.J. (1999). Inderdecadel climate variability in the northeast Pacific interpreted from the annual growth rings of mountain hemlock. Proceedings of the Workshop on Decoding Canada's Environmental Past: Adaption Lessons Based on Changing Trends and Extremes in Climate and Biodiversity. Edited by: D.C. MacIver. Downsview: Atmospheric Environment Service. p. 49-58.

Georgieva, K & Kirov, B. (2007). *Long-term variations in solar meridional circulation from geomagnetic data: implications for solar dynamo theory.*

Georgieva, K. & Kirov, B. (2006). *Long-term variations in solar meridional circulation from geomagnetic data: implications for solar dynamo theory.* Available online at: http://arxiv.org/ftp/physics/papers/0703/0703187.pdf

Georgieva, K., Kirov, B., Gavruseva, E. (2006). Geoeffectiveness of different solar drivers, and long-term variations of the correlation between sunspot and geomagnetic activity. *Physics and Chemistry of the Earth, 31, 81–87.*

Georgieva, K., Kirov, B. & Bianchi, C. (2005). Long-term variations in the correlation between solar activity and climate. *Mem. S.A.It. Vol. 76*, 965.

Georgieva, K & Kirov, B. (2005). *Helicity of Magnetic Clouds and Solar Cycle Variations of their Geoeffectiveness. Coronal and Stellar Mass Ejections Proceedings* IAU Symposium No. 226, 2005. K. P. Dere, J. Wang & Y. Yan, eds. 2005 International Astronomical Union.

Georgieva, K., Kirov, B., Gavruseva, E. & Javaraiah, J. (n.d.) Solar Differential Rotation and the Properties of Magnetic Clouds. Available online at http://arxiv.org/ftp/astro-ph/papers/0511/0511257.pdf

Georgieva, K., Kirov, B., Tonev, P., Guineva, V. & Atanasov, D. (n.d.) Solar activity: the importance of North-South solar activity asymmetry for atmospheric circulation. Available online at: *h*ttp://adsabs.harvard.edu/abs/2007AdSpR..40.1152G http://arxiv.org/ftp/physics/papers/0702/0702057.pdf

Georgieva, K. & Kirov, B. (2002). Long-term variations and interrelations of ENSO, NAO and solar activity. *Physics and Chemistry of the Earth, 27*, 441–448.

Georgieva, K & Kirov, B. (2000). Secular Cycle of the North-South Solar Asymmetry. *Bulgarian Journal of Physics 27 No. 2,* 28-34.

Georgieva, K. (1998). A relation between solar activity and temperature in Northern hemisphere in the period 1881–1988. *Bulg. Geophys. J. 3,* 114–119.

Grinsted, A., Moore, J. C. & Jevrejeva, S. (2004). Application of the cross wavelet transform and wavelet coherence to geophysical time series. *Nonlinear Processes in Geophysics 11:* 561–566.

Gross, R. S. (2005). The observed period and Q of the Chandler wobble, in *Forcing of Polar Motion in the Chandler Frequency Band: A Contribution to Understanding Interannual Climate Change*, edited by Plag, H. P., Chao, B. F., Gross, R. N. & van Dam, T. pp. 31-37, Cahiers du Centre Européen de Géodynamique et de Séismologie vol. 24, Luxembourg, 2005.

Gross, R. S. (2006). *Mass Transport and Dynamics in the Earth System: The Unsolved Scientific Questions and Observational Requirements.* Available online at: http://geodesy.unr.edu/ggos/ggosws_2006/position_papers/Gross_Position_Paper.pdf

Gross, R. S., Fukumori, I. & Menemenlis, D. (2005). Atmospheric and oceanic excitation of decadal-scale Earth orientation variations. *Journal Of Geophysical Research, vol. 110,* B09405, doi:10.1029/2004JB003565, 2005.

Haigh, J. D. (2007). *The Sun and the Earth's Climate*. http://www.livingreviews.org/lrsp-2007-2

Hansen, J., M.. Sato, and R. Ruedy, 1995. Long-term changes of the diurnal temperature cycle: Implications about mechanisms of global climate change. Atmos. Res. 37, 175-209.

Hsieh, W. W. (2004). Nonlinear Multivariate & Time Series Analysis by Neural Network Methods. *Review of Geophysics 42.* Available online at: http://www.ocgy.ubc.ca/~william/index.html

Hsieh, W. W. (2001). Nonlinear principal component analysis by neural networks. Appeared in *Tellus*, (2001), vol. 53A, pp. 599-615.

Hsieh, W. W. & Wu, A. (2002). Nonlinear characteristics of surface air temperature over Canada. submitted to *Journal of Geophysical Research (Atmosphere)* June 2001 accepted May 2002.

Hsieh, W. W. & Wu, A. (2001). Nonlinear multichannel singular spectrum analysis of the tropical Pacifc climate variability using a neural network approach. Submitted to *J. Geophys. Res. (Oceans),* April, 2001 Revised, Dec., 2001.

Hsieh, W. W. & Yuval. (n.d.) The impact of Time-Averaging on the detectabilty of nonlinear empirical relations. UBC. Available online at: http://www.ocgy.ubc.ca/~william/index.html

Holger, B., Christl, M., Rahmstorf, S., Andrey, Ganopolski, Augusto, et al. (2005). Possible solar origin of the 1,470-year glacial climate cycle demonstrated in a coupled model. Vol 438|10 November 2005|doi:10.1038/nature04121.

Jakob, M., McKendry, I. and Lee, R. (2003). Long–Term Changes in Rainfall Intensities
in Vancouver, British Columbia. *Canadian Water Resources Journal, 28(4).*

Javaraiah, J., Bertello, L. & Ulrich, R. K. (2005). Long-term variations in solar differential rotation and sunspot activity. *Solar Physics. 232 (1-2),* 25-40.

Javaraiah, J. (2003). '1.3-year' and '153-day' periodicities in the Sun's surface rotation. *Bulletin of the Astronomical Society of India 3,* 317-318.

Javaraiah, J. (2003). Long-term variations in the solar differential Rotation. *Solar Physics 212:* 23–49.

Jones, P. D. (1993). Hemispheric Surface Air Temperature Variations: A Reanalysis and an Update to 1993. *Journal of Climate Volume 7, Issue 11*. Available online at:http://ams.allenpress.com/archive/1520-0442/7/11/pdf/i1520-0442-7-11-1794.pdf http://ams.allenpress.com/perlserv/?request=get-abstract&doi=10.1175%2F1520-0442(1994)007%3C1794%3AHSATVA%3E2.0.CO%3B2

Jose, P. D. (1965). Sun's Motion and Sunspots. *The Astronomical Journal, Vol. 70, No. 3,* 193-200.

Juckett, D. (2000). Solar activity cycle, north/south asymmetries and differential rotation associated with solar spin-orbit variations, *Solar Phys., 191,* 201–226.

Juckett, D. (1998). Evidence for a 17-year cycle in the IMF directions at 1 AU, in solar coronal hole variations, and in planetary magnetospheric modulations. *Solar Physics 183(1):* 201-224.

Kaiser, D. P., (1998). Analysis of cloud amount over China, 1951-1994, *Geophysical Research Letters*, 25, 3599-3602.

Kalnay, E. & Cai, M. (2003). Impact of urbanization and land-use change on climate. *Nature 423,* 528-531.

Kane, R. P. (2002). Evolution of geomagnetic aa index near sunspot minimum. European Geosciences Union 2002. *Annales Geophysicae 20:* 1519–1527.

Karl, T. R., Jones, P. D. Knight, R. W., Kukla, G., Plummer, N. & Razuvayev, V., et al. (1993). A New Perspective on Recent Global Warming: Asymmetric Trends of Daily Maximum and Minimum Temperature. *Bulletin of the American Meteorological Society Volume 74, Issue 6.* Available online at: http://ams.allenpress.com/archive/1520-0477/74/6/pdf/i1520-0477-74-6-1007.pdf

Kato, C., Munakata, K., Yasue, S., Inoue, K. & McDonald, F. B. (2003). A ~1.7-year quasi-periodicity in cosmic ray intensity variation observed in the outer heliosphere. *Journal Of Geophysical Research, vol. 108, NO. A10,* 1367.

Keeling, C. D., Whorf, T. P. (2000). The 1,800-year oceanic tidal cycle: a possible cause of rapid climate change. *Proc Natl Acad Sci U S A. 97(8),* 3814-9.

Keeling, C. D. & Whorf, T. P. (1997). Possible forcing of global temperature by the oceanic tides. *Proc Natl Acad Sci U S A. 94(16):* 8321–8328. 1997, The National Academy of Sciences of the USA Colloquium Paper.

Keenlyside, N. S., Latif, M., Jungclaus, J., Kornblueh, L. & Roeckner, E. (2008). Advancing decadal-scale climate prediction in the North Atlantic sector. *Nature 453,* 84-88 doi:10.1038/nature06921; Received 25 June 2007; Accepted 14 March 2008; Corrected 8 May 2008

Kiffney, P.M., J.P. Bull and M.C. Feller. 2002. Climatic and Hydrologic Variability in a Coastal Watershed of Southwestern British Columbia. *Journal of the American Water Resources Association*, 38: 1437–1451.

Kniveton, D.R. & Todd M.C. (2001) On the relationship of cosmic ray flux and precipitation. *Geophysical Research Letters.,* 28 (8): 1527-1530

Kolaczek, B., Nastula, J. & Salstein, D. (2003). El Nino-related variations in atmosphere–polar motion interactions. *Journal of Geodynamics 36*, 397–406.

Knight, J. R., Allan, R. J. & Folland, C. K., Vellinga, M. & Mann, M. E. (2005). A signature of persistent natural thermohaline circulation cycles in observed climate. *Geophysical Research Letters, vol. 32.*

Krivova, N. A. & Solanki, S. K. (2002). The 1.3-year and 156-day periodicities in sunspot data: Wavelet analysis suggests a common origin. *Astronomy and Astrophysics 94(2):* 701-706.

Kumar, P. & Foufoula-Georgiou, E. (1997). Wavelet Analysis For Geophysical Applications. *Reviews of Geophysics, 35, 4* 385–412.

Landscheidt, T. (1995) *El Niño Forecast Revisited.* Available online at: http://www.john-daly.com/sun-enso/revisit.htm

Landscheidt, T. (2001 a) *Solar eruptions linked to North Atlantic Oscillation.* Available online at: http://www.john-daly.com/theodor/DecadalEnso.htm

Landscheidt, T. (2001 b) *Trends in Pacific Decadal Oscillation subjected to solar forcing.* Available online at: http://www.john-daly.com/sun-enso/revisit.htm.

Landscheidt, T. (2000 a): Solar forcing of El Niño and La Niña. *European Space Agency (ESA) Special Publication 463,* 135-140.

Landscheidt, T. (2000 b): River Po discharges and cycles of solar activity. Hydrol. *Sci. J. 45:*491-493.

Landscheidt, T. (2000 c): *Sun's role in the satellite-balloon-surface issue.* Available online: http://www.john-daly.com/solar/temps.htm

Landscheidt, T. (2000 d): *New confirmation of strong solar forcing of climate.* Available online at: http://www.john-daly.com/po.htm

Landscheidt, T. (2000 e). Solar wind near Earth: Indicator of variations in global temperature. *European Space Agency (ESA) Special Publication 463,* pp.497-500.

Landscheidt, T. (1999 a): Extrema in sunspot cycle linked to Sun's motion. *Solar Physics 189:* 413-424.

Landscheidt, T. (1999 b): Solar activity controls El Niño and La Niña. Available online: http://www.john-daly.com/sun-enso/sun-enso.htm

Landscheidt, T. (1998 a): Forecast *of global temperature, El Niño, and cloud coverage by astronomical means*. In: Bate, R., ed.: Global *Warming. The continuing debate.* Cambridge, The European Science and Environment Forum (ESEF), 172-183.

Landscheidt, T. (1998 b): Solar activity : A dominant factor in climate dynamics. Available: http://www.john-daly.com/solar/solar.htm

Landscheidt, T. (1995) *Global warming or Little Ice Age?* In: Finkl, C. W., ed.: *Holocene cycles. A Jubilee volume in celebration of the 80th birthday of Rhodes W. Fairbridge.* Fort Lauderdale, The Coastal Education and Research Foundation (CERF), 371-382.

Landscheidt, T. (1990). *Relationship between rainfall in the northern hemisphere and impulses of the torque in the Sun's motion*. In: K. H. Schatten and A. Arking, eds.: *Climate impact of solar variability*. Greenbelt, NASA, 259-266, 1990.

Landscheidt, T. (1988). Solar rotation, impulses of the torque in the Sun's motion, and climatic variation. *Climatic Change 12,* 265-295.

Landscheidt, T. (1987) *Long-range forecasts of solar cycles and climate change*. In: Rampino, M. R., Sanders, J. E., Newman, W. S. und Königsson, L. K., eds.: *Climate. History, Periodicity, and Predictability*. New York, van Nostrand Reinhold, 421-445.

Landscheidt, T. (1986 a) *Long-range forecast of energetic x-ray bursts based on cycles of flares.* In: Simon, P. A., Heckman, G. und Shea, M. A., eds.: *Solar-terrestrial predictions*. Proceedings of a workshop at Meudon, 18.-22. June 1984. Boulder, National Oceanic and Atmospheric Administration, 81-89.

Landscheidt, T. (1986 b) *Long-range forecast of sunspot cycles*. In: Simon, P. A., Heckman, G. und Shea, M. A., eds.: *Solar-terrestrial* *predictions.* Proceedings of a workshop at Meudon, 18.-22. June 1984. Boulder, National Oceanic and Atmospheric Administration, 48-57.

Landscheidt, T. (1983): *Solar oscillations, sunspot cycles, and climatic change*. In: McCormac, B. M., ed.: *Weather and climate responses to solar variations.* Boulder, Associated University Press, 293-308.

Landscheidt, T. (1976): Beziehungen zwischen der Sonnenaktivität und dem Massenzentrum des Sonnensystems. Nachrichten der Olbersgesellschaft 100, 2-19.

Lehmann, E., Leckebusch, G. C., Ulbrich, U. & Nevir, P. (2008). Effects of ENSO on sub-seasonal to interannual length-of-day (LOD) variability. *Geophysical Research Abstracts, Vol. 10*.

Leung, L.R. & Qian, Y. (2003). Changes in Seasonal and Extreme Hydrologic Conditions of the Georgia Basin/Puget Sound in an Ensemble Regional Climate Simulation for the Mid–Century. *Canadian Water Resources Journal, 28(4).* pp. 605-631.

Lewis, D.H. & Smith, D.J. (1999). *Little Ice Age climate trends at treeline in Strathcona Provincial Park, Vancouver Island: Insights from glaciers and trees.* Proceedings of the Workshop on Decoding Canada's Environmental Past: Adaption Lessons Based on Changing Trends and Extremes in Climate and Biodiversity. Edited by MacIver, D. C. Downsview: Atmospheric Environment Service. Issue 2, pp 19-30.

Liszka, L & Holmstr¨om, M. (1999). Extraction of a deterministic component from ROSAT X-ray data using a wavelet transform and the principal component analysis. *Astron. Astrophys. Suppl. Ser. 140,* 125-134.

Lockwood M. (2001). Long-term variations in the magnetic fields of the Sun and the heliosphere: Their origin, effects and implications. *Journal Geophysical Research*. 106, 16021-16038.

Lundstedt, H., Haigh, J. D. & Christiansen, F. (2007). Influence of Solar Activity Cycles on Earth's Climate. *Executive Summary Report.* ESTEC Contract no. 18453/04/NL/AR Issue 1, September 5, 2007.

Lundstedt, H., Liszka, L., Lundin, R. & Muscheler, R. (2006). Long-term solar activity explored with wavelet methods. *Ann. Geophys., 24,* 769–778.

Lundstedt, H. (2006*). Wavelet methods*. Swedish Institute of Space Physics, Lund. May 15, 2006.

Lundstedt, H. & Boberg, F. & Wintoft, P. (2006). Influence of Solar Activity Cycles on Earth's Climate. *Data Interpretation -- Solar -- Technical Note.*

Lundstedt, H. & Wintoft, P. (2006). Influence of Solar Activity Cycles on Earth's Climate. *Literary Survey on Sun-Earth Connections -- Solar Variability -- Technical Note*

Lundstedt, H., Liszka, L. & Lundin, R. (2005). Solar activity explored with new wavelet methods. European Geosciences Union 2005. *Annales Geophysicae, 23,* 1505–1511,

Makowski, K. Wild, M., Ohmura, A. (2008). Diurnal temperature range over Europe between 1950 and 2005. *Atmos. Chem. Phys. Discuss*., 8, 7051-7084, 2008 http://www.atmos-chem-phys-discuss.net/8/7051/2008/acpd-8-7051-2008.html

McKinnell, S. M. & and Crawford, R. W. (2007). The 18.6-year lunar nodal cycle and surface temperature variability in the northeast Pacific, *Journal Of Geophysical Research, 112,* C02002.

McCracken, K. G., Dreschhoff, G. A. M., Smart, D. F. & and Shea, M. A. (2001). The Gleissberg periodicity in large fluence solar proton events. Proceedings of ICRC 2001: 3205.

Meehl, G.A., Zwiers, F. W., Knutson, T., Mearns, L. O. & Whetton, P. (2000). Trends in Extreme Weather in Climate Events: Issues Related to Modeling Extremes in Projection of Future Climate Change. *Bulletin of the American Meteorological Society, 81:* 427-436.

Mekis, E. & Hogg, W. D. (1999). Rehabilitation and Analysis of Canadian Daily Precipitation Time Series. *Atmosphere-Ocean 37 (1)* 53–85.

Ministry of Environment, British Columbia. (2007). *Environmental Trends in British Columbia: 2007*. www.env.gov.bc.ca/soe/et07

Ministry of Environment, British Columbia ,(2006). British Columbia's Coastal Environment: 2006. Available online at: www.env.gov.bc.ca/soe/bcce/

Ministry of Forests and Range, British Columbia. (2006). Preparing for Climate Change: Adapting to Impacts on British Columbia's Forest and Range Resources.

Ministry of Environment, British Columbia (1993).Trends. Available online at: http://www.env.gov.bc.ca/soerpt/files_to_link/trends1993/whole_report.pdf

Ministry of Land, Water, & Air Protection, British Columbia. (2002). Indicators of Climate Change for British Columbia 2002.

Mishra, R. A. & Mishra, R. K. (2005). Effect of solar heliospheric parameters and geomagnetic activity on long-term cosmic ray anisotropy. 29th International Cosmic Ray Conference Pune (2005) 00, 101-104

Mishra, R. K. & Mishra, R. A. (2007). Cosmic Ray Anisotropy and Solar Activity. *Brazilian Journal of Physics, vol. 37, no. 4,* 1227

Mackey, R. (2007). Rhodes Fairbridge and the idea that the solar system regulates the Earth's climate. *Journal of Coastal Research,* SI 50 (Proceedings of the 9th International Coastal Symposium), 955 – 968. Gold Coast, Australia, ISSN 0749.0208

Mayaud, P. N. (1972). The aa indices: A 100 year series characterizing the magnetic activity. *Journal of Geophysical Research 77,* 6870-6874.

Moberg, A., Philip, D. Jones, D.L., Walther, A., Brunet, M., Jacobeit, J., Alexander, L.V., Della-Marta, P.M., Jürg Luterbacher, & Yiou, P. (2006), Indices for daily temperature and precipitation extremes in Europe analyzed for the period 1901–2000, *J Geophys Res,* 111, D22106, doi:10.1029/2006JD007103. http://www.agu.org/pubs/crossref/2006/2006JD007103.shtml http://www.geo.uni-augsburg.de/de/lehrstuehle/phygeo/personal/jacobeit/

Moore, R.D. & I.G. McKendry (1996). "Spring Snowpack Anomaly Patterns and Winter Climatic Variability, British Columbia, Canada". Water Resources Research, 32(3): 623–632.

Mote, P.W. (2003). Twentieth–Century Fluctuations and Trends in Temperature,

Precipitation and Mountain Snowpack in the Georgia Basin–Puget Sound Region. *Canadian Water Resources Journal, 28(4).*

Mursula, K. & Hiltula, T. (2008). Systematically Asymmetric HeliosphericMagnetic Field: Evidence for a QuadrupoleMode and Non-axisymmetry with Polarity Flip-flops. Kluwer Academic Publishers. pp. 567-585

Mursula, K. (2007). Bashful ballerina: The asymmetric Sun viewed from the heliosphere. *Advances in Space Research 40*. 1034–1041.

Mursula, K. & Vilppola, J. H. (2004). Fluctuations of the solar dynamo observed in the solar wind and interplanetary magnetic field at 1AU and in the outer Heliosphere, *Solar Phys., 221,* 337–349.

Mursula, K., Zieger, B., & Vilppola, J. H. (2003). Mid-term periodicities in geomagnetic activity during the last 15 solar cycles: Connection to solar dynamo strength, *Solar Phys., 212,* 201–207.

Mursula, K., Hiltula, T. & Zieger, B. (2002). Latitudinal gradients of solar wind speed around the ecliptic: Systematic displacement of the streamer belt. *Geophysical Research Letters, Vol. 29, No. 15,* 1738, 10.1029/2002gl015318, 2002.

Mursula, K., Vernova, E. S., Tyasto, M. I. & Baranov, D. G. (2002). A New Pattern For the North–South Asymmetry of Sunspots. *Solar Physics 205:* 371–382.

Mursula, K & Zieger, B. (2001). Long-term north-south asymmetry in solar wind speed inferred from geomagnetic activity: A new type of century-scale solar oscillation? *Geophysical Research Letters Vol. 28, No. 1,* -98.

Mursula, K. & Zieger, B. (1999). Simultaneous occurrence of mid-term periodicities in solar wind speed, geomagnetic activity and cosmic rays, Proc. of the Cosmic Rays Conference, Utah, 7, pp. 123-126, 17–25 August 1999.

Mursula, K. & Zieger, B. (1998). Solar excursion phases during the last 14 solar cycles. *Geophysical Research Letters, Vol. 25, No. 11,* 1851-1854.

Mursula, K. & Zieger, B. (1998). Annual variation in near-Earth solar wind speed: Evidence for persistent north-south asymmetry related to solar magnetic polarity. Geophysical Research Letters, Vol. 25, No. 6, Pages 841-844.

Mursula, K. & Ulich, T. H. (1998). A new method to determine the solar cycle length. *Geophysical Research Letters, Vol. 25, No. 11, 1837-1840.*

Mursula, K. & Zieger, B. (1996). The 13.5 Day Periodicity in the Sun, Solar Wind, & Geomagnetic Activity: The Last Three Solar Cycles. *Journal of Geophysical Research Vol. 101 No*. A12.

Mursula, K. and Hiltula, T., Bashful ballerina: Southward shifted heliospheric current sheet, Geophys. Res. Lett.,30, 2, 2003. doi: 10.1029/2003GL018201.

Nesme-Ribes, E., Baliunas, S. L. & Sokoloff, D.: The stellar dynamo. *Scientific American*. August 1996, 51-52.

Newman, M., Compo, G. P. & Alexander, M. A. (2003). ENSO-Forced Variability of the Pacific Decadal Oscillation. *Journal Of Climate - Letters 16(23):* 3853-3857.

Nigam, S., M. Barlow, & E. H. Berbery (1999). Analysis Links Pacific Decadal Variability to Drought and Streamflow in the United States.

EOS, Transactions, American Geophysical Union, Vol 80, No. 51, Dec 21 1999.

Pallé, E & Butler, C. J. (2004). The proposed connection between clouds and cosmic rays: cloud behaviour during the past 50–120 years, *J. Atmosph. Solar-Terr. Phys. 64,* 327–337.

Pallé, E., Goode, P. R., Montanes-Rodriguez, P. & Koonin, S. E. (2004). Changes in Earth's reflectance over the past two decades. *Science* 304(): 1299-1301.

Pallé, E., Butler, C, J. & O'Brien, K. (2004). The possible connection between ionization in the atmosphere by cosmic rays and low level clouds. *Journal of Atmospheric and Solar-Terrestrial Physics* 66 1779–1790.

Palle, E. & Butler, C.J. (2001). Sunshine records from Ireland: Cloud factors and possible links to solar activity and cosmic rays *International Journal of Climatology*.21 (6): 709-729

Palus, M. & Novotna, D. (2007). Common oscillatory modes in geomagnetic activity, NAO index and surface air temperature records. *J. Atmospheric and Solar-Terrestrial Physics.* Available online at: http://www.cs.cas.cz/mp/papers07/novotnamod2pr.pdf

Paluš, M., Kurths, J., Schwarz, U., Seehafer, N., Novotná, D. & Charvátová, I. (2007). The solar activity cycle is weakly synchronized with the solar inertial motion. *Physics Letters A 365*, 421–428.

Peralta-Hernandez, A.R., Balling R.C, & Barba-Martinez, L.R. (2008), Analysis of near-surface diurnal temperature variations and trends in southern Mexico*, International Journal of Climatology.* Available online at: http://www3.interscience.wiley.com/journal/119755413/abstract?CRETRY=1&SRETRY=0

Perry, C.A. (2007). Evidence for a physical linkage between galactic cosmic rays and regional climate time series. *J. Adv. Space Res*. doi:10.1016/j.asr.2007.02.079, J. Adv. Space Res. (2007). Available online at: http://ks.water.usgs.gov/waterdata/climate/c.perry.asr2007.pdf

Pielke, R.A., Davey, A.C., Dev Niyogi, Souleymane Fall, Steinweg-Woods, J. Hubbard, K., Lin, X., Cai, M., Lim, Y. & Li , H.(2007), Unresolved issues with the assessment of multidecadal global land surface temperature trends, J Geophys Res, 112, D24S08, doi:10.1029/2006JD008229. http://www.agu.org/pubs/crossref/2007/2006JD008229.shtml

Pines, D. & Shaham, J. (1973). Seismic Activity, Polar Tides and the Chandler Wobble. *Nature* 245, 77 - 81

Reid, G.C. (1997). Solar forcing of global climate change since the mid-17th century. *Climatic Change*. Vol.37, No.2, pp.391-405.

Reid, G. C. (1987). Influence of solar variability on global sea surface temperatures. *Nature* Vol 329 pp. 142-143.

Richardson, J. D., Paularena, K. I., Belcher, J. W. & Lazarus, A. J. (1994). Solar wind oscillations with a 1.3 year period. Da Silva, R. R. & Avissar, A. (2005). The impacts of the Luni-Solar oscillation on the Arctic oscillation. *Geophysical Research Letters, Vol. 32,* L22703, Doi:10.1029/2005gl023418, 2005. Available online at: ftp://space.mit.edu/pub/plasma/publications/jdr_per/jdr_per.withthumbs.pdf

Rogers, M. L., Richards, M. T. & Richards, D. P. (2006). Long-Term Variability In The Length Of The Solar Cycle. *Astro-Physics.*

Rohde, R. A., & Muller, R. A. (2005). Cycles in fossil diversity. *Nature,* Vol. 434, pp. 208-210.

Rouillard, A & Lockwood, M. (2004). Oscillations in the open solar magnetic flux with a period of 1.68 years: imprint on galactic cosmic rays and implications for heliospheric shielding. *Annales Geophysicae 22:* 4381–4395.

Sakurai, T. (2002). Eleven-year solar cycle periodicity in sky brightness observed at Norikura, Japan. *Earth Planets Space, 54,* 153–157.

Scafetta, N. & West, B. J. (2005). Estimated solar contribution to the global surface warming using the ACRIM TSI satellite composite. *Geophysical Research Letters Vol. 32.*

Scafetta, N. & West, B. J. (2006). Phenomenological solar signature in 400 years of reconstructed Northern Hemisphere temperature record. *Geophysical Research Letters, vol. 33,* l17718,.

Scafetta, N. & West, B. J. (2006). Phenomenological solar contribution to the 1900-2000 global surface warming*. Geophysical Research Letters, VOL. 33,* L05708, doi:10.1029/2005GL025539, 2006

Scherer, K., Fichtner, H., Heber, B., Ferreira, S. E. S., Potgieter, M. S. (2008). Cosmic ray flux at the Earth in a variable heliosphere. *Advances in Space Research 41* (2008) 1171–1176.

Shahinaz, M. & Yousef. (2000). *The Solar Wolf-Gleissberg Cycle and its Influence on the Earth.* ICEHM2000, Cairo University, Egypt, September, 2000, page 267- 293.

Shaviv, N. R. (2005). On climate response to changes in the cosmic ray flux and radiative budget. *Journal of Geophysical Research* v.110, A08105, 2005 doi:10.1029/2004JA010866. Available online at: http://arxiv.org/PS_cache/physics/pdf/0409/0409123v1.pdf

Shaviv, N. J. (n.d.). Cosmic rays diffusion in the dynamic milky way: model, measurement and terrestrial effects. Available online at: http://www.phys.huji.ac.il/~shaviv/articles/ShavivErice.pdf

Shaviv, N. R.& Veizer, J. (2003). Celestial Driver of Phanerozoic Climate? *GSA Today 13:7,* 4-10.

Shaviv, N. R. (2002). Cosmic Ray Diffusion from the Galactic Spiral Arms, Iron Meteorites, and a Possible Climatic Connection. *Phys. Rev. Lett. 89,* 051102 (2002)

Smadi, M. M. (2006). Observed Abrupt Changes in Minimum and Maximum Temperatures in Jordan in the 20th Century. *American Journal of Environmental Sciences 2 (3):* 114-120.

Smith, D. J. & Laroque, C. P. (1998). Mountain Hemlock Growth Dynamics on Vancouver Island. Pages 67-70 in J.A. Trofymow and A. MacKinnon, editors. Proceedings of a workshop on Structure, Process, and Diversity in Successional Forests of Coastal British Columbia, February 17-19, 1998, Victoria, British Columbia. *Northwest Science, Vol. 72 (special issue No. 2).*

Smith, D. J. & Laroque, C. P. (1999). Tree-ring analysis of yellow-cedar (Chamaecyparis nootkatensis) on Vancouver Island, British Columbia. Can. J. For. Res. 29: 115–123 (1999).

Smith, D. J. & Laroque, C. P. (1998). High-Elevation Dendrochronological Records from Vancouver Island. Decoding Canada's Environmental Past. *Proceedings of the Workshop on Decoding Canada's Environmental Past: Climate Variations and Biodiversity Change during the Last Millennium.* Edited by: D.C. MacIver and R.E. Meyer. Downsview: Atmospheric Enviroment Service. p. 33-44.

Stone D., Weaver, A.J. (2002), Daily Maximum and Minimum Temperature Trends in a Climate Model, *Geophys. Res. Lett., 29 (9),* 1356.

Stone, D. A. and Weaver, A. J. (2003). Factors contributing to diurnal temperature range trends in twentieth and twenty-first century simulations of the CCCma coupled model, *Climate Dynamics, 20,* 435-445.

Stuck, J., Seitz, F. & Thomas, M. (2005). Atmospheric forcing mechanisms of polar motion. In: Plag, H.-P.; Chao, B.F.; Gross, R.; van Dam, T. (Eds.), *Proceedings of the workshop: Forcing of polar motion in the Chandler frequency band: a contribution to understanding interannual climate variations.,* European Seismological Commission, 127-133.

Svalgaard, L. & Cliver, E.W. (n.d.). Long-term Geomagnetic Indices and their Use in Inferring Solar Wind Parameters in the Past. Available online at: http://www.leif.org/research/ISSC06-43-Svalgaard.pdf

Svensmark, H. & Enghoff, M. B. (2008). The role of atmospheric ions in aerosol nucleation – a review. *Atmos. Chem. Phys. Discuss., 8,* 7477–7508.

Svensmark, H. (2007) a. Cosmoclimatology: a new theory emerges. *Astronomy & Geophysics, Volume 48, Issue 1* (p 1.18-1.24).

Svensmark, H., Pedersen, J.O.P., Marsh, N.D., Enghoff, M.B., Uggerhoj, U.I. (2007) b. Experimental evidence for the role of ions in particle nucleation under atmospheric conditions*. Proc. R. Soc. A 463,* 385–396.

Svensmark, H. (2006). Cosmic rays and the biosphere over 4 billion years. *Astron. Nachr*. / AN 327, No. 9, 871 – 875 (2006) .

Marsh, N.D. & Svensmark, H. (2003) Solar Influence on Earth's Climate. *Space Sci. Rev., 107,* 317–325.

Marsh, N.D. & Svensmark, H. (2000) *Low Cloud Properties Influenced by Cosmic Rays,* Phys. Rev. Lett., 85, 5004–5007.

Tatiana V., Barlyaeva, Dmitri, I & Ponyavin. (n.d.). Solar Signal in climate change: Cross Wavelet and EMD analysis of time--series. Available online at: http://www.esa-spaceweather.net/spweather/workshops/eswwII/proc/Session2/Poster_2ESWW_Barlyaeva_and_Ponyavin.pdf

Thejil, P. & Lassen, K. (1999). Solar Forcing of the Northern Hemisphere Land Temperature: New Data. *Danish Meteorological Institute. Scientific Report 99-9.*

Tinsely, B. A. (2000). Influence of Solar Wind on the Global Electric Circtuit, and Inferred Effects on Cloud Micriphysics, Temperature, and Dynamics in the Troposphere. *Space Science Reviews 00:* 1–28.

Tinsley, B.A. & Yu, F. (2004). *Atmospheric Ionization and Clouds as Links Between Solar Activity and Climate.*

Tinsley, B.A. & Roldugin, V.C. (2004). Atmospheric transparency changes associated
with solar wind-induced atmospheric electricity variations. *J. Atmos. Solar Terrestrial Phys. 66,* 1143–1149.

Tinsley, B. A., Burns, G. B. & Zhou, L. (2007). The role of the global electric circuit in solar and internal forcing of clouds and climate. *Advances in Space Research 40* 1126–1139.

Tinsley, B. A. & Kniveton, D. R. (n.d.)Daily changes in global cloud cover and Earth transits of the heliospheric current sheet. Available online at: http://www.utdallas.edu/nsm/physics/pdf/tin_dcgcc.pdf

Tinsley, B. A. (1997). Do effects of global atmospheric electricity on clouds cause climatic changes? *EOS*, 19. August 1997, 341, 344, 349.

Tiwari, C. M., Tiwari, D. P., Pandey, A. K. & Shrivastava, P. K. (2005). Average Anisotropy Characteristics of High Energy Cosmic Ray Particles and Geomagnetic Disturbance Index Ap. J. Astrophys. Astr. (2005) 26, 429–434.

Tomes, R. (2005). The 154 day solar cycle and related cycles. *Cycles Research Institute*

Torrence, C. & Compo, G. P. (1998). A Practical Guide to Wavelet Analysis. *Bulletin of the American Meteorological Society. Vol. 79, No. 1, January 1998.*

Torrence, C and Compo, G. P. (1997). *A Practical Guide to Wavelet Analysis.* submitted to the Bull. Amer. Met. Soc., May 1, 1997 revised July 28, 1997.

Tung, K. & Camp, C. D. (2007). Surface warming by the solar cycle as revealed by the composite mean difference projection. *Geophysical Research Letters Vol. 34,* L14703 2007.

Tung, & Coughlin, K. T. (2004). 11-Year solar cycle in the stratosphere extracted by the empirical mode decomposition method. *Advances in Space Research 34,* 323–329.

Tung, K. & Coughlin, K. T. (2005). *Empirical Mode Decomposition of Climate Variability (Chapter 7 of book).* Available online at: http://www.amath.washington.edu/research/articles/Tung/journals/coughlin-tungHHT05.pdf

Turner, R.J.W. & Clague, J. J. (1999). Temperature Rising – Climate Change in Southwestern British Columbia. *Addendum to Volume I, Canada Country Study, Environment Canada / Geological Survey of Canada, Miscellaneous Report 67.*

Usoskin, I. G. & Gennady, A., Kovaltsov. (2008). Cosmic rays and climate of the Earth: possible connection. *C. R. Geoscience 340* 441–450.

Usoskin, I. G. & Kovaltsov, G. A. (2007). Regional cosmic ray induced ionization and geomagnetic field changes. *Adv. Geosci., 13,* 31–35.

Usoskin, I. G., Gennady, A & Kovaltsov. (2006). Link between cosmic rays and clouds on different time scales. Advances *in Geosciences, Volume 2: Solar Terrestrial (ST).* Editor-in-Chief: Wing-Huen I. P. Volume Editor-in-Chief: Duldig, M. ISBN: 981-256-985-5 (ISBN for the set of 5 volumes: 981-256-456-X). Published by World Scientific Co., Pte. Ltd., Singapore, 2006, pp.321-331.

Usoskin, I. G., Voiculescu, M., Kovaltsov, G. A. & Mursula, K. (2006). Correlation between clouds at different altitudes and solar activity: Fact or Artifact? *Journal of Atmospheric and Solar-Terrestrial Physics 68* 2164–2172.

Usoskin, I. G., Marsh, N., Kovaltsov, G. A., Mursula, K. & Gladysheva. O. G. (2004). Latitudinal dependence of low cloud amount on cosmic ray induced ionization. *Geophysical Research Letters, Volume 31, Issue 16,* CiteID L16109

Vaccaro, J.J. (2002). Interdecadal Changes in the Hydrometeorological Regime of the Pacific Northwest and in Regional–Hemispheric Climate Regimes and their Linkages. U.S. Geological Survey. *Water Resources Investigations Report 02*–4176.

Valdés-Galicia, J. F., Velasco, V. M. & Mendoza, B. (2005). Mid Term Cosmic Ray Quasi Periodicities And Solar Magnetic Activity Manifestations. 29th International Cosmic Ray Conference Pune (2005) 00, 101-104.

Valdés-Galicia, J. F., Pérez-Enríquez, R. & Otaola, J. A. (1996). The cosmic-ray 1.68-year variation: A clue to understand the nature of the solar cycle? *Solar Physics, 167,* 409-417.

Valev, D. (2006). Statistical relationships between the surface air temperature anomalies and the solar and geomagnetic activity indices. *Physics and Chemistry of the Earth 31* 109–112.

Veizer, J. (2008). Climate, water and CO2: a geological perspective. *Mineralogical Magazinev, 72; no. 1; p. 293-294*.

Veizer, J. (2005). Celestial Climate Driver: A Perspective from Four Billion Years of the Carbon Cycle. *Geoscience Canada, Volume 32, Number .* Available online at: http://www.sciencebits.com/files/articles/GACV32No1Veizer.pdf

Veretenenko, S. V., Dergachev, V. A. & Dmitriev, P. B. (2007). Effect of solar activity and cosmic-ray variations on the position of the Arctic front in the North Atlantic. *Volume 71, Number 7*.

Vieira, L. E., Rigozo, N. R., Echer, E., Nordemann. (2001). Geomagnetic-solar Activity Correlation Evolution. D. J. *American Geophysical Union, Spring Meeting 2001. 05/2001.*

Vincent, L. A. & Mekis, E. (2006). Changes in Daily and Extreme Temperature and Precipitation Indices for Canada over the Twentieth Century. *Atmosphere-Ocean 44 (2)*, 177–193.

Vincent, L. A., Zhang, X., Bonsal, B. R. & Hogg, W. D. (2001). Homogenization of Daily Temperatures over Canada. *Journal of Climate Vol 15* p.1322-1334.

Vincent, L. A., Peterson, T. C., Barros, V. R., Marino, M. B., Rusticucci, M. Carrasco, et al. (2005). Observed Trends in Indices of Daily Temperature Extremes in South America 1960–2000. *Journal Of Climate 18:* 5011-5023.

Vilppola, J. (2003). Solar Wind: Detection Methods And Long-Term Fluctuations. *University Of Oulu Report Series In Physical Sciences Report No. 26.*

Vondrák, J., Ron, C. (2005). The Great Chandler Wobble Change in 1923–1940 Re-Visited. Available online at: http://66.102.1.104/scholar?num=30&hl=en&lr=&q=cache:WwBoI7_uHBgJ:www.sbl.statkart.no/literature/plag_etal_2005_editors/vondrak_final.ps+author:j+author:vondrak

Vondrák, J. (1999). Earth rotation parameters 1899.7–1992.0 after reanalysis within the hipparcos frame. *Surveys in Geophysics 20:* 169–195.

Vondrák, J. (1985). Long-period behaviour of polar motion between 1900.0 and 1984.0. *Annales Geophysicae (ISSN 0755-0685), vol. 3,* p. 351-356.

Vose, R. S., Easterling, D. R. & Gleason, B. R. (2005), Maximum and minimum temperature trends for the globe: An update through 2004, *Geophys. Res. Lett., 32,* L23822, doi:10.1029/2005GL024379.

Vukcevic, M. A. (2004). Synchronising effect of planetary resonance. Available online at: http://hal.archives-ouvertes.fr/docs/00/00/19/81/PDF/solar_synchronisation.pdf

Vukcevic, M. A. (2004). Evidence of a multi resonant system within solar periodic activity. Available online at: http://arxiv.org/ftp/astro-ph/papers/0401/0401107.pdfWade, N.L., Martin, J. & Whitfield, P. H. (2001). Hydrologic and Climatic Zonation of Georgia Basin, British Columbia. *Canadian Water Resources Journal, 26(1):* 43-70.

Walker, I.R. & Pellatt, M. G. (2003). Climate Change in Coastal British ColumbiaA Paleoenvironmental Perspective. *Canadian Water Resources Journal,* 28(4). Weather, Climate, & the Future: BC's Plan. (2004).

Walters, J. T., McNider, R.T., Shi, X., Norris, W.B. & Christy, J.R. (2007), Positive surface temperature feedback in the stable nocturnal boundary layer, *Geophys Res Lett*, 34, L12709. http://www.agu.org/pubs/crossref/2007/2007GL029505.shtml

Wendler, J. (2004). External forcing of the geomagnetic field? Implications for the cosmic ray flux—climate variability. *Journal of Atmospheric and Solar-Terrestrial Physics 66* 1195– 1203.

Wild, M., Atsumu O., & Makowski, K. (2007), Impact of global dimming and brightening on global warming, *Geophys Res Lett*, 34, L04702.

White, W. B., Lean, J., Cayan, D. R. & Dettinger, M. D. (1997). Response of global upper ocean temperature to changing solar irradiance, J. Geophys. *Res., 102(C2),* 3255–3266.

Whitcher, B., Guttorp, P. & Percival, D. B. (2000). Wavelet Analysis of Covariance with Application to Atmospheric Time Series. To appear in *Journal of Geophysical Research - Atmospheres 2000.*

Whitcher, B., Guttorp, P. & Percival, D. B. (n.d.) Mathematical Background for Wavelet Estimators of Cross-Covariance and Cross-Correlation. *NRCSE Technical Report Series NRCSE-TRS No. 038.* Available online at: http://www.nrcse.washington.edu/pdf/trs38_wavelet.pdf

Whitfield, P.H., Wang, J. H. & Cannon, A. J. (2003). Modelling Future Streamflow

Extremes – Floods and Low Flows in Georgia Basin, British Columbia. *Canadian Water Resources Journal, 28(4).* Available online at: 27(4): 427-456

Whitfield, P. H., Reynolds, C. J. & Cannon, A. J. (2002). Modelling Streamflow in Present and Future Climates: Examples from the Georgia Basin, British Columbia. *Canadian Water Resources Journal Vol. 27, No. 4, 2002.*

Wilson, I. R. G., Carterand, B. D. & Waite, I A. (2008). Does a Spin–Orbit Coupling Between the Sun and the Jovian Planets Govern the Solar Cycle? *Publications of the Astronomical Society of Australia, 25(2)*, 85–93.

Wilson, I.R.G. (2007). Do periodic peaks in the planetary tidal forces acting upon the sun influence the solar cycle? Available online at: http://ozwx.plasmaresources.com/wilson/Syzygy.pdf

Wilson, I. R. G. (2006). Possible Evidence of the de Vries, Gleissberg and Hale Cycles in the Sun's Barycentric Motion. *Australian Institute of*

Physics 17th National Congress 2006 – Brisbane, 3-8 December 2006. RiverPhys Paper No. XXX.

Wilson, R. J. S. & Luckman B. H. (2003). Tree-ring reconstruction of maximum and minimum temperatures and the diurnal temperature range in British Columbia, *Canada. Dendrochronologia, Volume 20, Number 3,* 257-268 (12).

Wilson, R. M. (1998). Evidence for solar-cycle forcing and secular variation in the Armagh Observatory temperature record (1844-1992). *Journal of Geophysical Research 103(D10):* 11159-11171.

Wilson, R., R., D'Arrigo, B., Buckley, U., Büntgen, J., Esper, D., Frank, B., Luckman, S., Payette, R., Vose D., & Youngblut, D. (2007), A matter of divergence: Tracking recent warming at hemispheric scales using tree ring data, J Geophys Res, 112, D17103, doi:10.1029/2006JD008318. http://www.agu.org/pubs/crossref/2007/2006JD008318.shtml

Yiou, P., Sornette, D. & Ghil, M. (2000). Data-adaptive wavelets and multi-scale singular-spectrum analysis. *Physica D, 142,* 254–290.

Yndestad, H. (2006). The influence of the lunar nodal cycle on Arctic climate. ICES *Journal of Marine Science: Journal du Conseil 2006 63(3):*401-420.

Zhong, Y. (2005). Coupled Response of Global Climate to Solar Cycle Forcing. Center for Climatic Research. *CCR Internal Working Report #1. Contribution Number: 917.*

Zhou, Liming, Aiguo Dai, Yongjiu Dai, Russell S. **Vose**, Cheng-Zhi Zou, Yuhong Tian, and Haishan Chen (2008), Spatial dependence of diurnal temperature range trends on precipitation from 1950 to 2004, *Climate Dyn*amics. Available online at: http://www.springerlink.com/content/n67n8447p60466h7